EUROPEAN COMMISSION

Community research

BELBaR

(Contract Number: 295487)

DELIVERABLE

2nd Annual WORKSHOP 16th-18th June, 2014
Parkhotel du Sauvage, Meiringen (Switzerland)

AGENDA & Collection of abstracts

Date of issue of this report: **30/06/14**

Start date of project: **01/03/12** Duration: 48 Months

Project co-funded by the European Commission under the Seventh Euratom Framework Programme for Nuclear Research &Training Activities (2007-2011)		
Dissemination Level		
PU	Public	X
RE	Restricted to a group specified by the partners of the BELBaR project	
CO	Confidential, only for partners of the BELBaR project	

EURATOM

Participants list:

	Participant	Institution	Nation	E-Mail
1	Katerina Videnska	UJV Rez	Czech Republic	katerina.videnska@ujv.cz
2	Radek Cervinka	UJV Rez	Czech Republic	radek.cervinka@ujv.cz
3	Rasmus Eriksson	B+Tech	Finland	rasmus.eriksson@btech.fi
4	Tim Schatz	B+Tech	Finland	tim.schatz@btech.fi
5	Pirkko Hölttä	Helsinki Univ.	Finland	pirkko.holtta@helsinki.fi
6	Seppo Kasa	POSIVA	Finland	seppo.kasa@posiva.fi
7	Fionán O'Carroll	Saanio & Riekkola Oy	Finland	fionan.ocarroll@sroy.fi
8	Nuria Marcos	Saanio & Riekkola Oy	Finland	nuria.marcos@sroy.fi
9	Michal Matusewicz	VTT	Finland	michal.matusewicz@vtt.fi
10	Veli-Matti Pulkkanen	VTT	Finland	veli-matti.pulkkanen@vtt.fi
11	Harald Zänker	HZDR-IRE	Germany	h.zaenker@hzdr.de
12	Stephan Weiss	HZDR-IRE	Germany	s.weiss@hzdr.de
13	Florian Huber	KIT-INE	Germany	florian.huber@kit.edu
14	Frank Friedrich	KIT-INE	Germany	frank.friedrich@kit.edu
15	Franz Rinderknecht	KIT-INE	Germany	franz.rinderknecht@kit.edu
16	Thorsten Schäfer	KIT-INE	Germany	thorsten.schaefer@kit.edu
17	Vladimir Petrov	MSU	Russia	vladimir.g.petrov@gmail.com
18	Tiziana Missana	CIEMAT	Spain	tiziana.missana@ciemat.es
19	Ursula Alonso	CIEMAT	Spain	ursula.alonso@ciemat.es
20	Magnus Hedström	Claytech	Sweden	mh@claytech.se
21	Guomin Yang	KTH	Sweden	guomin@kth.se
22	Ivars Neretnieks	KTH	Sweden	niquel@kth.se
23	Luis Moreno	KTH	Sweden	lm@kth.se
24	Christian Nystrom	SKB	Sweden	christian.nystrom@skb.se
25	Patrick Sellin	SKB	Sweden	patrik.sellin@skb.se
26	Jinsong Liu	SSM	Sweden	Jinsong.Liu@ssm.se
27	Andrew J. Martin	NAGRA	Switzerland	andrew.martin@nagra.ch
28	Florian Kober	NAGRA	Switzerland	florian.kober@nagra.ch
29	Daniel Grolimund	PSI-SLS	Switzerland	daniel.grolimund@psi.ch
30	Paul Smith	SAM Ltd.	Switzerland	paul@sam-ltd.com
31	Lucy Bailey	NDA	UK	lucy.bailey@nda.gov.uk
32	Rebecca Beard	NDA	UK	rebecca.beard@nda.gov.uk
33	Nick Bryan	Univ. Manchester	UK	nick.bryan@manchester.ac.uk
34	Nicholas Sherriff	Univ. Manchester	UK	nicholas.sherriff@manchester.ac.uk
35	Christopher Reid	University of Strathclyde	UK	christopher.reid@strath.ac.uk

AGENDA

Monday June 16th: Individual arrival

Tuesday June 17th:

9:00- 9:30	Welcome, Introduction and background (P. Sellin, Chr. Nyström, T. Schäfer)
9:30 – 10:15	Invited talk: **Daniel Grolimund** (PSI-SLS): *"Colloid mobilization and colloid facilitated transport in natural porous media: phenomena and modeling"*
10:15 - 10:20	Overview & current status WP1: "Safety Assessment" (NDA)
10:20 – 10:40	***Coffee/Tea***
10:40 - 10:45	Overview & current status WP2: "Erosion" (CIEMAT)
10:45 - 11:10	**Rasmus Erikson** (B+Tech): *"Progress update on rheological studies"*
11:10 - 11:35	**Magnus Hedström** (Claytech): *"Update on erosion experiments"*
11:35 - 11:55	**Michal Matusewicz** (VTT): *"MX-80 micro structure at different densities"*
11:55 - 12:25	**Tim Schatz** (B+Tech): *"Update on artificial fracture tests at B+Tech & Status of Artificial Fracture Benchmark Tests"*
12:30 - 14:00	***Lunch***
14:00 – 14:20	**Christopher Reid** (Univ. Strathclyde) *"Understanding the role of accessory minerals in buffer erosion migitation"*
14:20 - 14:40	**Frank Friedrich** (KIT-INE): *"Update on erosion experiments studies and characterization of released material"*
14:40 - 15:00	**Tiziana Missana** (CIEMAT): *"Progress update of CIEMATS laboratory results"*
15:00 - 15:05	Overview & current status WP3: "Radionuclide & host rock interaction" (KIT-INE)
15:05 – 15:25	**Pirkko Hölltä** (HU): *"Radionuclide sorption on MX-80 bentonite colloids and colloid associated radionuclide transport"*
15:25 – 15:45	**Katerina Videnska** (UJV): *"Study of Sr-85 transport through a column fill with crushed granite in presence of bentonite colloids"*
15:45 – 16:05	**Nick Bryan** (Univ. Manchester): *"Radionuclide/Bentonite dissociation kinet ics"*
16:05 – 16:30	***Coffee/Tea***
16:30 – 16:50	**Thorsten Schäfer** (KIT-INE): *"New results from the CFM project & current status"*
16:50 – 16:55	Overview & current status WP4: "Colloid stability" (UJV)
16:55 – 17:15	**Harald Zänker** (HZDR-IRE): *"Actinide(IV) colloids at near-neutral pH due to reaction with dissolved silicic acid"*
17:15 - 17:35	**Radek Cervinka** (UJV): *"Coagulation behavior of clay dispersions in presence of various cations, anions and organic matter"*

19:00 ***Dinner***

Wednesday June 18th:

9:00 – 9:05 Overview & current status WP5: "Conceptual & mathematical models" (POSIVA)

9:05 – 9:25 **Veli-Matti Pulkannen** (VTT): "Modelling slit erosion experiments"

9:25 – 9:45 **Florian Huber** (KIT-INE): "Status update of the modeling work"

9:45 – 10:05 **Ivars Neretnieks** (KTH): *"Bentonite expansion and Erosion – development of a two-region model"*

10:05 - 10:25 **Guomin Yang** (KTH): *"Theoretical studies with DFT on Ca/Na- bentonite: structure, forces & swelling properties"*

10:25 – 11:00 Overview & current status WP6: "Dissemination" & WP7 "Coordination" (SKB)

11:00 - 11:30 *Coffee* /Tea

11:30 - 12:30 Topical discussion meeting (2-3 Topics): *Status since the last meeting*

1) Bentonite erosion benchmark test on artificial fractures
2) Clay Colloids and geochemistry – what is the relation?
3) Predictive modelling tools – the way forward

12:30 - 12:45 Summary (SKB)

12:45 – 13:30 Transfer to Grimsel Test Site; GTS (*lunch boxes will be provided*)

13:30 – 15:45 Visit Grimsel Test Site

Back transfer to Meiringen train station to catch the 16:41h train to Zurich Airport (arrival Zurich Airport 19:13h)

COLLOID MOBILIZATION AND COLLOID FACILITATED TRANSPORT IN NATURAL POROUS MEDIA: PHENOMENA AND MODELLING

Daniel Grolimund [1*], Kurt Barmettler [2], Michal Borkovec [3]

[1] Swiss Light Source, microXAS Beamline Project, Paul Scherrer Institute, Villigen PSI, (CH)
[2] Institute of Terrestrial Ecology, Swiss Federal Institute of Technology, Zurich (CH)
[3] Analytical and Biophysical Environmental Chemistry, University of Geneva, Geneva (CH)

* Corresponding author: daniel.grolimund@psi.ch

Abstract

Mobile colloidal particles have been identified to be involved in a broad variety of environmentally relevant processes [1-4]. A considerable number of these processes may have hazardous consequences. Most recently, mobile colloidal particles have been reported to be a potentially relevant transport pathway for strongly sorbing contaminants [5-8]. Thereby the colloidal particles act as highly mobile contaminant carries and enhance in such a way the spreading of sorbing pollutants in subsurface systems. Therefore, considering potential hazardous incidents due to mobilized colloidal particles should represent a critical task in risk assessment of any subsurface contamination problem, in the development of remediation strategies, as well as in recharge and waste water management. In order to judge or predict the susceptibility of a subsurface system to the phenomena of enhanced contaminant transport by mobile colloidal particles, a detailed understanding of the following processes is required [4]: (i) the generation of mobile colloidal particles, (ii) the life-time of these particles within the system, and (iii) the association of the contaminant with the mobile particles. In the present paper various aspects of the diverse problem of enhanced contaminant transport by *in-situ* mobilized colloid particles will be addressed.

A comprehensive set of laboratory-scale column experiments was performed in order to investigate relevant fundamental processes such as particle mobilization, particle deposition and transport, as well as multicomponent contaminant transport phenomena. In addition, dynamic light scattering techniques were used to study the aggregation behavior of *in-situ* mobilized colloidal particles over a wide range of solution conditions. Complementary analytical techniques were applied in order to enlighten the physical and chemical properties of the mobilized particles. The knowledge about structure and dynamic of each process obtained by these individual experimental investigations were compiled and incorporated into an extended contaminant transport model. The resulting set of coupled, non-linear partial differential equations was solved numerically and used to simulate and analyze contaminant transport experiments where *in-situ* mobilized colloidal particles have been proven to be a dominant transport pathway [6].

Information about the general nature of the particle release process was obtained by studying mobilization phenomena in natural porous media under well-controlled conditions. A pronounced non-exponential release behavior, the finite supply of colloidal particles and the strong dependence of the observed release kinetic on chemical system parameters turn out to represent general characteristics of the release process. The non-exponential release behavior

can be rationalized in terms of a broad distribution of populations of particles. This heterogeneity of the colloidal particles initially present in the system results in characteristic release pattern [7,8]. Further, as a consequence of the sensitivity of the release process on the present chemical conditions, a distinct interplay between mobilization of colloidal particles and multicomponent transport phenomena could be established. An illustrative example is depicted in Figure 1. The outflow pattern for an experiment with variations in the ionic strength and simultaneous presence of different components (sodium and calcium) is shown. The sequence of feed solutions is summarized in Figure 1a. The corresponding breakthrough patterns of sodium and calcium are shown in a semilogarithmic representation in Figure 1b. The breakthrough behavior of these two major cations governs the particle release pattern shown in Figure 1c. Each reduction in ionic strength results in a sudden increase of the particle concentration in the outflow. Furthermore, the observed tail of this peak ends abruptly with the arrival of the retarded exchange front (compare course of the calcium concentration, Figure 1b).

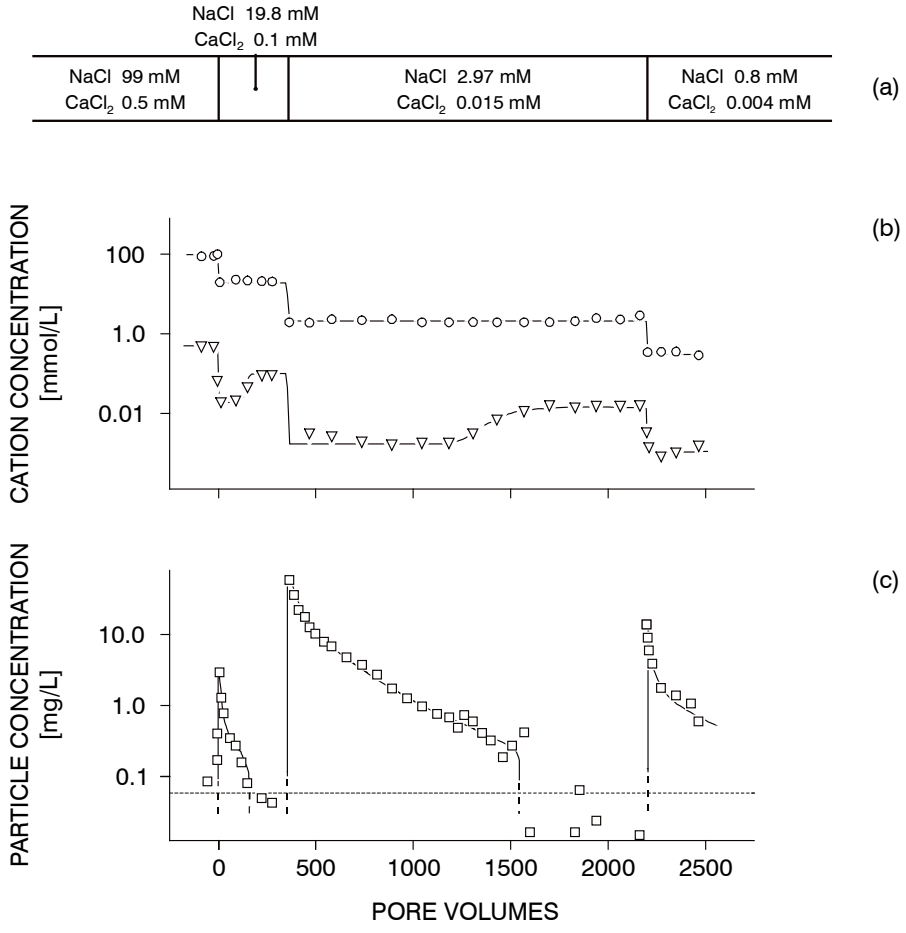

Figure 1: Release of colloidal particles in the simultaneous presence of sodium and calcium. The feed solutions (a) contain a constant sodium/calcium molar ratio of 200:1. The mobilization is induced by step-wise changes in normality. (b) Resulting outflow pattern of sodium and calcium in a semi-logarithmic scale. (c) Concentration of colloidal particles suspended in the outflow in a semi-logarithmic representation. In spite of the presence of divalent cations in the outflow mobilization of particles can be observed.

After mobilization, the life-time of colloidal particles is mainly determined by convective transport, particle (re-)deposition, and the aggregation behavior. The morphology and structure of the porous media influences the convective transport of the mobile particles which can be distinctly different from a conservative tracer. The processes of particle (re-)deposition and aggregation turned out to be dominantly influenced by solution chemistry as well as the surface chemical properties of the colloidal particles and the porous media. As an example, the influence of the electrolyte concentration, counterion valence, and solution pH on the deposition rate coefficient is shown in Figure 2.

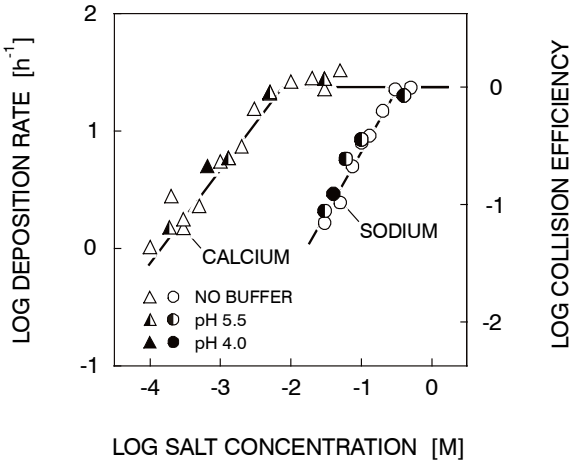

Figure 2: Influence of solution chemistry on particle deposition kinetics in packed soil columns. Effect of electrolyte (NaCl or $CaCl_2$) concentration, counterion valence (Na^+ and Ca^{2+}), and solution pH (pH 4.0 or 5.5, controlled by azide buffer) on deposition rate coefficients and experimental collision efficiencies for *in-situ* mobilized soil particles in their parent porous medium.

The three processes of particle mobilization, deposition and aggregation occur in general simultaneously. However, the relative importance of each of these processes is strongly dependent on the present chemical and physical conditions.

An extended transport model considering colloidal phenomena was formulated based on various independent experiments, each focusing on one particular process in an isolated fashion. This model was successful in the description of coupled multicomponent transport and particle mobilization phenomena taking place simultaneously in a natural porous media. This modeling attempt clearly demonstrated the pronounced impact of ionic strength, solution and surface composition on particle release rates. Furthermore, the model was able to predict the observed breakthrough pattern of complex contaminant transport experiments, including the phenomena of enhanced contaminant transport by *in-situ* mobilized colloidal particles.

In conclusion, experiments and model calculation clearly demonstrated the potential importance of *in-situ* mobilized colloidal particles as a predominant transport vector of contaminants in natural subsurface systems. The experimentally simulated situations and the observed processes are likely to be operational in the field. Nevertheless, one has to be careful in trans-

lating the results obtained in laboratory column studies into actual field situations. Additional systematic investigations concerning mobilization and transport phenomena including natural, heterogeneous systems as well as well-characterized model systems are needed. Especially the combination of experimental investigations and mathematical modelling corresponds to a powerful tool in order to achieve a refined understanding of the chemical or physical system parameters controlling particle release under field conditions. Such efforts would result in an improved ability to understand and predict the susceptibility of natural systems for hazardous phenomena induced by mobilized colloidal particles such as enhanced transport of contaminant associated with mobile particles.

References:

[1] Jenny, H.; Smith, G. D. *Soil Sci.* **1935**, 39, 377-389.
[2] Muecke, T. W. *Journal of Petroleum Technology* **1979**, 31, 144-150.
[3] Khilar, K. C.; Fogler, H. S. *Reviews in Chemical Engineering* **1987**, 4, 41-108.
[4] Ryan, J. N.; Elimelech, M. Colloids and Surfaces A. **1996**, 107, 1 - 56.
[5] Vinten, A. J. A.; Yaron, B.; Nye, P. E. *J. Agric. Food Chem.* **1983**, 31, 662 - 664.
[6] Grolimund, D.; Borkovec, M.; Barmettler, K.; Sticher, H. *Environ. Sci. Technol.* **1996**, 30, 3118-3123.
[7] Grolimund, D.; Borkovec M. Water Resour. Res., **2001,** 37, 559-570.
[8] Grolimund, D.; Barmettler, K.; Borkovec M. *Water Resour. Res.,* **2001,** 37, 571-582.

PROGRESS UPDATE ON RHEOLOGICAL STUDIES

Rasmus Eriksson[1*], Tim Schatz1[1]

[1] B+Tech (FIN)

* Corresponding author: rasmus.eriksson@btech.fi

Abstract

One scenario of interest for repository safety assessment involves the erosive loss of bentonite buffer material in contact with dilute groundwater flowing through a transmissive fracture interface. Material that extrudes into a fracture develops a concentration gradient that may lead to erosive loss of material at the extrusion front. In order to further examine the sol/gel transition behavior observed in artificial fracture tests at the extrusion/erosion interface, a series of rheological experiments on sodium and calcium montmorillonite suspensions covering a range of solids contents spanning from the "swelling paste" phase (15 vol-%) to the sol phase (0.1 vol-%) were initiated.

The results demonstrate that both sodium and calcium montmorillonite arrange into attractive structures, albeit with very different properties. Sodium montmorillonite tends to form volume-spanning, elastic, gel-like structures, while calcium montmorillonite tends to form dense flocs that exhibit only weak elastic response and low yield stress (at low solids content, <8 vol-%). Considering a scenario where erosion is possible, it means that buffer extrusion into a fracture may be quite different, mechanistically, depending on whether the counter ion population is dominated by sodium or calcium. Thus it can be expected that a dense gel-like phase extrudes into the fracture if sodium dominates and a porous, weakly gel-like, structure extrudes into the fracture if calcium dominates. Obviously, the permeability of the extruding phase may differ considerably between these two cases, which, for instance, could have consequences on possible radionuclide migration, etc.

We also compared the strength of the montmorillonite gels to the expected shear forces exerted on the gels by flowing groundwater and for most systems it is extremely unlikely that shear forces can break the gel structures. Only pure calcium montmorillonite form weak enough gels that may could potentially break due to groundwater flow. On the other hand, experiments have shown that calcium montmorillonite does not tend to erode, which can be explained by its tendency to flocculate into large heavy agglomerates that sediment.

UPDATE ON EROSION EXPERIMENTS

Magnus Hedström[1*], Emelie Hansen [1**]

[1] Clay Technology AB (SWEDEN)

* Corresponding author: mh@claytech.se
** Now at BASF A/S, Copenhagen (DENMARK)

Abstract

An update on the erosion experiments performed at Claytech will be given. These experiments are performed in a flow-through artificial fracture made of poly(methyl methacrylate). As there is plenty of support that montmorillonite in sodium form present the worst case with regard to erosion under low-salinity conditions, all the experiment reported here are performed using homoionic Wyoming Na-montmorillonite (Wy-Na). The origin of the montmorillonite used is MX-80 bentonite. Two different apertures of the artificial fracture have been used, 120 μm and 240μm. The erosion rate has been measured at a range of flow rates and at salinities varying from deionized water to 20 mM NaCl (aq), which is the critical coagulation concentration Wy-Na. The phase diagram for Wy-Na has also been determined and we will se how that connects to the erosion behaviour.
Furthermore, we have noticed a strong hysteresis effect, namely that erosion rates at a given NaCl concentration of the flowing water depends on weather the concentrations are increased or decreased. Increasing concentrations erosion stops at 15 mM NaCl, but on deceasing concentrations erosion does not start until the concentration in the flowing solution is as low as 5 mM.
Some comparisons with similar experiments (see BELBaR Deliverable D2.5) performed at B+ Tech Oy, ÚJV Řež, a.s. and KIT-CN/INE will also be presented. When the systems are not homoionic, ion exchange may take place. How to handle this issue will also be discussed.

MX-80 MICROSTRUCTURE AT DIFFERENT DENSITIES

Michał Matusewicz[1*], Andrew Root[2], Veli-Matti Pulkkanen[1], Markus Olin[1]

[1] VTT Technical Research Centre of Finland (FI)
[2] MagSol (FI)

* Corresponding author: michal.matusewicz@vtt.fi

Abstract

The microstructure of water saturated MX-80 bentonite is investigated using a set of complimentary methods. Transmission electron microscopy (TEM) is used to provide qualitative images of the clay, small angle X-ray scattering (SAXS), ion exclusion (IE) and nuclear magnetic resonance (NMR) give information about the pore structure of the clay. A set of samples with density ranging from 0.7 to 1.6 g/cm^3 equilibrated either with water or with 0.1M sodium perchlorate is investigated. A test comparison of the influence of way of preparation of the sample on the structure is reported.

Introduction

The microstructure of the bentonite clay changes with the change of the density (eg. Holmboe et al., 2012, Muurinen, 2009) and of the water content (eg. Villar et al., 2012). Investigation of water saturated samples poses numerous experimental problems. To the best of our knowledge currently there is no method allowing direct and full characterization of the microstructure of swelling clay. Therefore we use a set of complimentary methods: transmission electron microscopy (TEM) to provide qualitative images of the clay, small angle X-ray scattering (SAXS), ion exclusion (IE) and nuclear magnetic resonance (NMR) to give information about the pore structure of the clay.

Research work description in brief

TEM imaging
Thin, 90 nm sections of epoxy embedded clay are imaged at magnification between 690 to 98000 times. Obtained shadowgraphs give the intuitive view of the clay from micro to nanoscale.

Porosity structure
Three methods are employed to divide pore water in the bentonite. SAXS gives the interlamellar distance and therefore can be used to estimate the volume of interlamellar pores. IE measures amount of anions entering the clay and so estimating the pore volume available for anions. Variable temperature NMR experiments divide water by the relaxation time of hydrogen nuclei after excitation with electromagnetic pulse. This depends on their surroundings, i.e. water in smaller pores give different signal than water in the bigger pores.

Influence of wetting
A brief test of influence of pre-wetting on the structure was run. Two samples of dry density 1.6 g/cm^3, one dry, one water saturated, were allowed to swell to 0.7 g/cm^3 dry density. Differences in the SAXS spectra were noted between the samples.

Acknowledgement

TEM imaging was carried out in the EM Unit of the Institute of Biotechnology at Helsinki University. Financial support from the VTT Graduate School is acknowledged (M.M.).

References

Holmboe, M., Wold, S. & Jonsson, M. (2012) Porosity investigation of compacted bentonite using XRD profile modeling. *Journal of contaminant hydrology,* **128**, 1–4, pp. 19-32.

Muurinen, A. , 2009-42. (2009), Studies on the Chemical Conditions and Microstructure in the Reference Bentonites of Alternative Buffer Materials Project (ABM) in Äspö. Posiva OY, Eurajoki. 1-46 p.

Villar, M.V., Gómez-Espina, R. & Gutiérrez-Nebot, L. (2012) Basal spacings of smectite in compacted bentonite. *Applied Clay Science,* **65–66**, 0, pp. 95-105.

List of Abbreviations

TEM - transmission electron microscopy
SAXS - small angle X-ray scattering
IE - ion exclusion
NMR - nuclear magnetic resonance

UPDATE ON ARTIFICIAL FRACTURE TESTS AT B+TECH

Tim Schatz[1]

B+Tech Oy, Laulukuja 4, 00420 Helsinki, Finland

* Corresponding author: tim.schatz@btech.fi

Experiments probing buffer erosion in fracture environments under flow-through conditions relative to buffer composition, groundwater composition, flow velocity, accessory minerals, fracture geometry and fracture surface roughness are ongoing at B+Tech.

Results to be presented and discussed at the BELBaR 2nd Annual Workshop include:

- The effect of fracture slope angle on erosion.

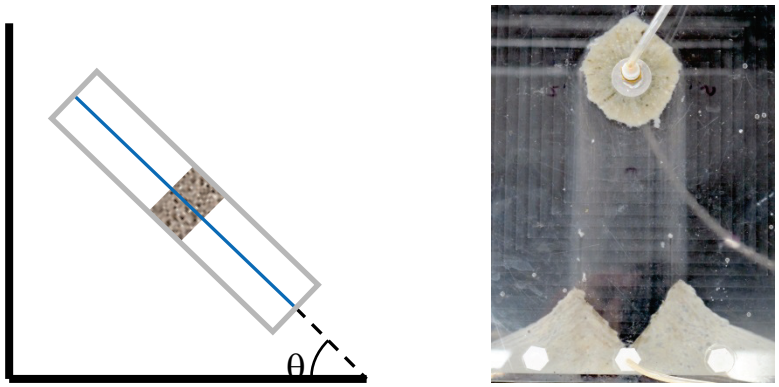

Figure 1. *Schematic diagram (left) showing artificial fracture test system positioned at steep slope angles (θ ≥ 45°) and MX-80 bentonite (right) in contact with a Grimsel groundwater simulant at an average flow rate of 0.09 ml/min down a 1 mm aperture artificial fracture system positioned at a 45° slope angle after 144 h.*

- The effect of montmorillonite composition on erosion.

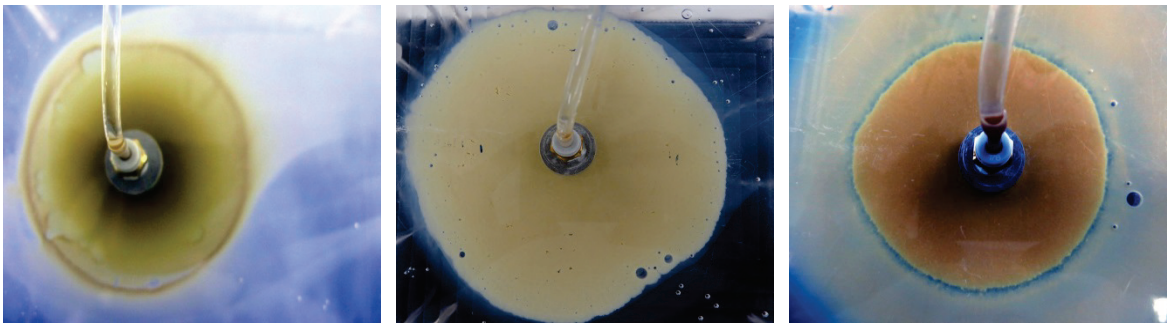

Figure 2. *Overhead images of tests with sodium montmorillonite from MX-80 bentonite (left), Milos bentonite (middle) and Kutch bentonite (right) against Grimsel groundwater simulant flowing in a 1 mm aperture fracture at an average flow rate of 0.09 ml/min.*

- The effect of surface roughness on erosion.

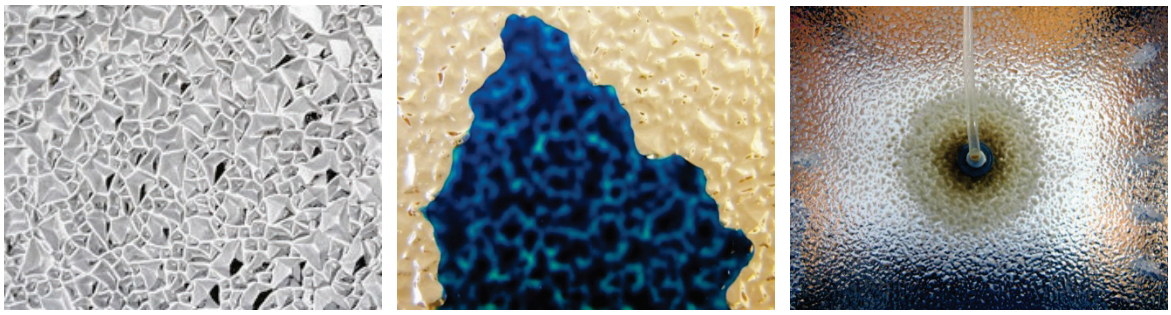

Figure 3. *Images* of *structured acrylic material (left) used to cover the upper and lower fracture surfaces in the rough-walled, artificial fracture system, aliquot of blue dye between two such fracture plates (middle) and test with sodium montmorillonite in contact with deionized water in the rough-walled, artificial fracture system after approximately 600 h (right).*

Additionally, the application of Optical Coherence Tomography (OCT), a three dimensional *in situ* imaging technique, and Magnetic Resonance Imaging (MRI) to erosion in the artificial fracture environment will be introduced.
The status of the BELBaR artificial fracture benchmark test program will also be discussed.

UNDERSTANDING THE ROLE OF ACCESSORY MINERALS IN BUFFER EROSION MIGITATION

Christopher Reid[1*], Rebecca Lunn[1], Alessandro Tarantino[1], Grainne El Mountassir[1]

Department of Civil and Environmental Engineering University of Strathclyde, Glasgow, UK

* Corresponding author: christopher.reid@strath.ac.uk

Abstract

Upon the intrusion of dilute glacial melt water to repository depth, and subsequent erosion of extruded bentonite buffer material from transmissive fractures, it has been proposed that the accessory minerals present within the buffer may form a protective porous filter, effectively straining montmorillonite colloids and mitigating against further release (Neretnieks et al 2009).
In order to test this theory, a flow through fracture cell 26cm in diameter was constructed by casting a natural fracture present in a granite core using clear rigid epoxy resin.

Figure 1: *Depiction of casting process.*

The fracture's complimentary face was cast repeating steps 1 & 2 depicted in figure 1. Inlet and outlet ports and a central compartment to house a compacted bentonite plug were recessed in the plates. The top plate was off-set slightly to create a naturally variable fracture aperture before the plate was sealed. The hydraulic aperture of the cell was then established by flowing water through the cell at a constant flow rate, measuring the head difference across the cell and applying the cubic law. The hydraulic aperture was found to be 190 µm. Holes to bolt the cell together and lock it in place at this aperture were then drilled. An Omega LCM302 – 2KN button load cell was also employed on the underside of the fracture to monitor swelling pressure throughout the test. The cell is illustrated in figure 2:

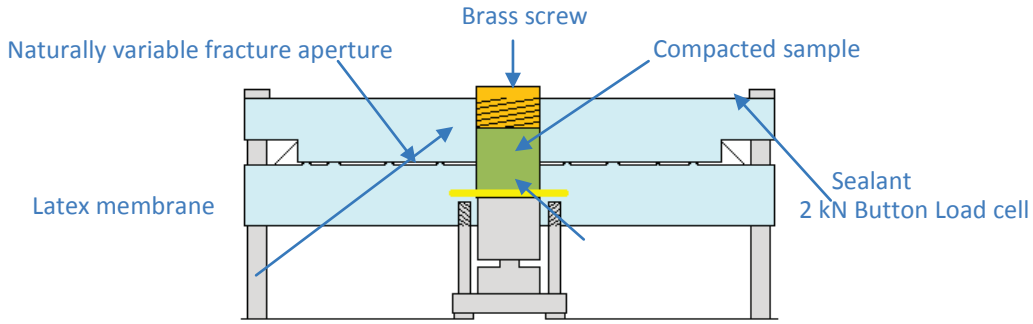

Figure 2: *Illustration of cell housing compacted sample*

As delivered, MX-80 buffer material was compacted to $\rho_d = 1650kg/m^3$ at a *water content = 18%*. The resultant pellet had a *height = 1cm* and *diameter = 2cm*. The pellet was installed in the fracture and flow through commenced at a constant flow rate of 1ml/min. Gravimetric analysis was undertaken on the effluent, sampling at 24 hour intervals and filtering through a 0.2 µm filter. Time lapse image capture was also undertaken for the purpose of quantitative image analysis.

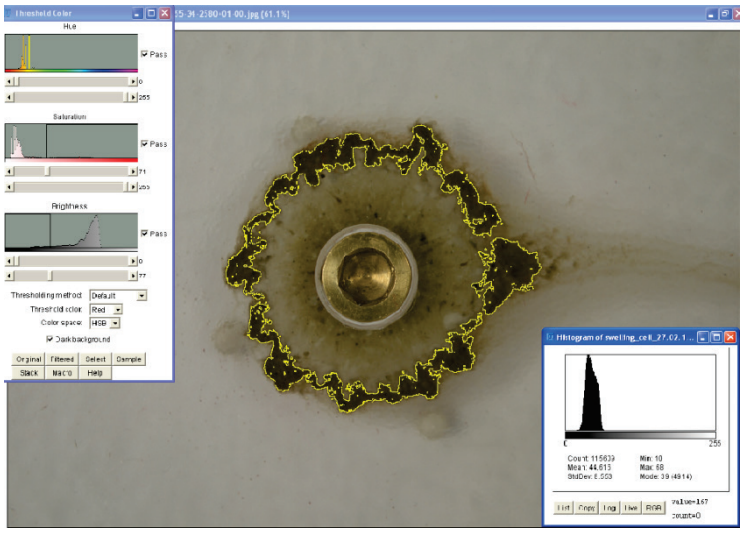

Figure 3: *Example of extruded bentonite material and image analysis undertaken on accessory mineral ring.*

To date, the test has been running for 105 days and erosion rate data appears to exhibit a cyclical nature. This shall be discussed along with the way in which erosion rate data correlates with image analysis and swelling pressure data.

References

Neretnieks, I., Liu, L., Moreno, L. (2009) Mechanisms and models for bentonite erosion. SKB report TR-09-35

UPDATE ON EROSION EXPERIMENTS AND CHARACTERIZATION OF RELEASED MATERIAL

Frank Friedrich, Franz Rinderknecht, Thorsten Schäfer

Karlsruhe Institute of Technology (KIT) Institute for Nuclear Waste Disposal (INE), Hermann-von-Helholtz-Platz 1, 76344 Eggenstein-Leopoldshafen, Germany

In this study the erosion and swelling behaviour of the FEBEX bentonite has been investigated during erosion experiments conducted in a custom-made flow through cell. Its housing is made of acrylic glass, has a diameter of 18 cm and an aperture of 1 mm. For the tests compacted FEBEX bentonite rings (inner diameter: 4 cm, outer diameter 8 cm, height: 2.5 cm) were used (initial density: 1650 kg/m^3). The rings were placed in a cavity in the center of the cell and subsequently hydrated after closure of the cell. Grimsel groundwater was pumped through the cell by a peristaltic pump with an initial flow velocity $v_{init.} = 10^{-5}$ m/s. Furthermore this cell was equipped with a pressure sensor (disynet XP1103-A1-100BG) to monitor the evolution of the bentonite swelling pressure during the experiment (Fig. 1a).

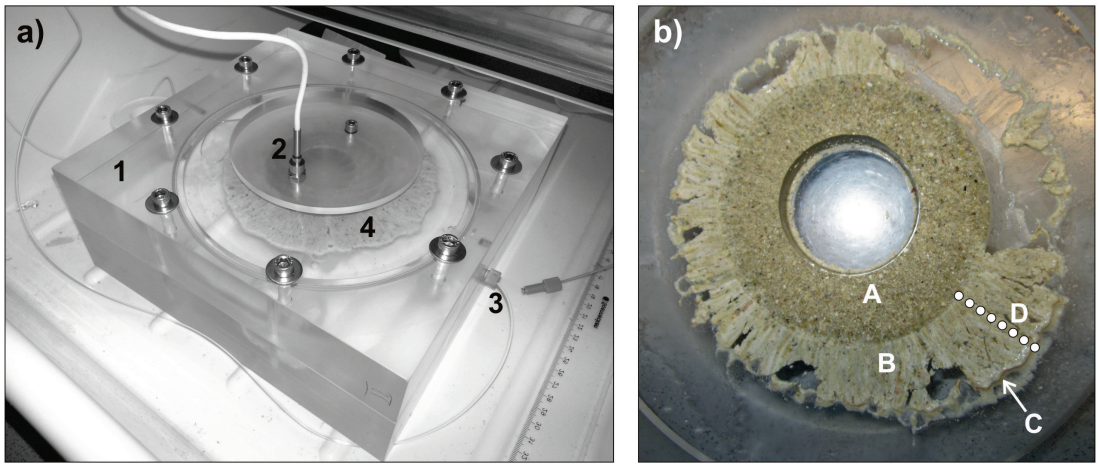

Figure 1: *a) setup of the flow through cell; visible are the acrylic glass housing (1), the pressure sensor (2) with the (dark) bentonite ring beneath, the water inlet (3) and the erosion halo (4). b) Halo of eroded material around the bentonite ring. (A) compacted bentonite ring, (B) eroded material, (C) gel layer, (D) sample locations for XRD measurements.*

Within the first 24 h after the start of the experiment the swelling pressure rises up to 2.6 MPa (Figure 2a). During the following days the pressure decreases to a constant value between 1.7 to 1.8 MPa implying steady state conditions (Fig. 2b). This pressure drop coincides with the bentonite swelling into the 1 mm aperture.

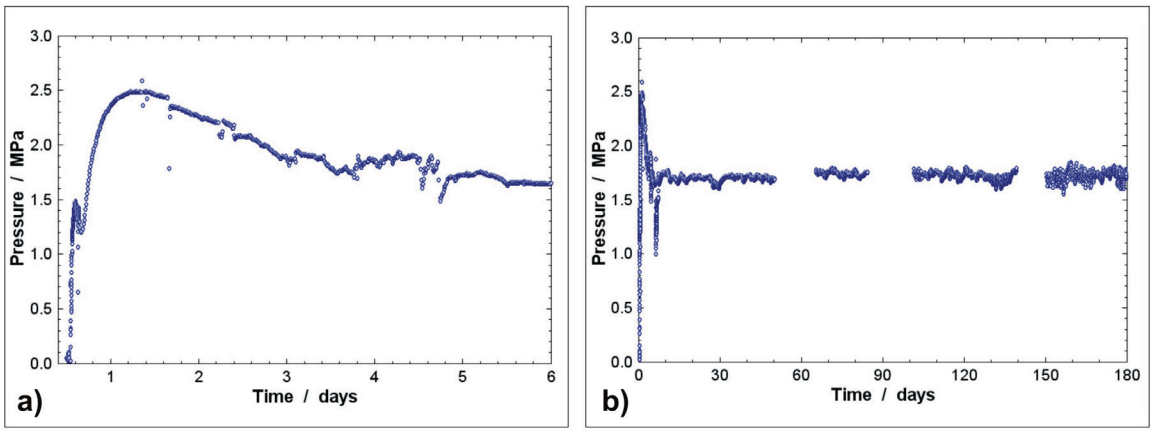

Figure 2: *Results of pressure measurements over a time period of 180 days.*

In the course of the experiment a "halo"-like structure of eroded material was formed within the 1 mm aperture, which did not expand anymore after 40 days and had a final diameter of 2 – 2.5 cm. The experiment was stopped and the eroded material was sampled along a traverse from the outermost part (gel layer) to the bentonite ring, in total eight samples were taken (Fig. 1b).

The X-ray diffractometric analysis of the gel layer shows, that not only clay minerals like montmorillonite and traces of illite are eroded, but also feldspars (orthoclase, plagioclase) and quartz particles migrate far into the outer parts of the erosion halo (Fig. 3a), while carbonates like calcite and dolomite where only detected in the inner halo parts (Fig. 3b).

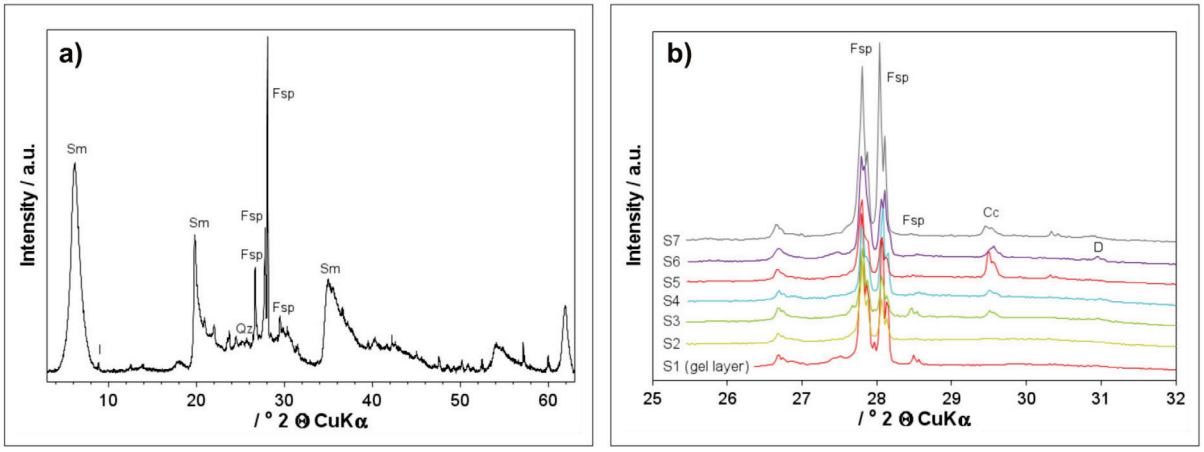

Figure 3: *X-ray patterns of halo samples. a) XRD pattern of the gel layer, showing peaks of smectite, feldspars and traces of illite and quartz. b) patterns of the samples S1 (gel layer) to S7 (contact to ring) showing peaks in the range from 25 – 32° 2Θ. Carbonates can be detected close to the compacted ring, but not in the gel layer.*

Furthermore scanning electron micrographs show strongly agglomerated clay material and unexpectedly large sizes for feldspar and quartz grains, lying in the range of 10 – 50 µm even in the gel layer.

PROGRESS UPDATE OF CIEMAT'S LABORATORY RESULTS

Tiziana Missana*, Ursula Alonso, Miguel García-Gutiérrez, Natalia Mayordomo, Ana Benedicto

* tiziana.missana@ciemat.es

Abstract

The presentation will summarize research conducted at CIEMAT during the last year within the BELBaR Project. The obtained results are mainly related to the workpackages: WP2 "Erosion" and WP4 "Colloid stability".
In particular, CIEMAT work has been focused on the following topics:

a) Characterisation of different bentonite (and saponite) clays, to gather information on their chemical and structural properties for the analysis of their possible implications on erosion processes.
b) Erosion experiments with different bentonites (under favourable conditions). Information on this topic and the previous one is also available in the Deliverable D2.4
c) Analysis of the irreversibility of the colloid coagulation processes. Information on this topic is also available in the Deliverable D4.4.
d) Analysis of the effects of the presence of different anions on colloid stability.

1. Characterisation of different bentonite clays and analyses of their erosion behaviour.

Five bentonites, from different origins, were analysed to gather information on their chemistry, mineralogy, accessory minerals, cations present in the interlayer; cation exchange capacity, pore water chemistry, charge distribution, cell formula, etc…,

This characterization is needed for the interpretation of erosion tests and a better understanding of erosion mechanisms. The selected bentonites were: FEBEX from Spain; IBECO from Mylos in Greece; Wyoming MX-80 from USA; Czech Rokle Na-activated (B75) and a Russian bentonite from the Khakassia deposit.

The colloidal properties (surface potential, zetapotential, and mean hydrodynamic size) and the coagulation as a function of pH and ionic strength were studied for all the bentonites (and a Spanish saponite). Then, their erosion behaviour was analysed.
Erosion experiments were carried out with raw bentonites compacted at 1.65 g/cm^3 and using deionised water to obtain maximum colloid erosion; the used experimental set-up has been previously used by CIEMAT. Clay colloid formation is monitored by periodical sampling of 2 mL of the contacting aqueous phase for colloid size distribution and colloid concentration measurements, by Photon Correlation Spectrometry (PCS).
Results showed that the higher mass of colloids detached corresponded to the Febex bentonite, slightly lower in MX-80 and Ibeco clay and lower for the other clays. In this comparison, smectite content (higher in the Febex case), rather than to the exchangeable Na (higher in MX-80, seems to be important for erosion. Further analyses will be carried out in the future.

2. Analysis of the irreversibility of the colloid coagulation process.

Bentonite erosion is expected when the chemical conditions favor colloid stability but in an "aggregated" system the formation of particles of colloidal size is not. Most of stability studies dealt with the analysis of colloid coagulation but much less is known on the reverse process: i.e. the "disaggregation". Nevertheless to evaluate the (ir)-reversibility of the coagulation process and its kinetic, when the conditions of the aqueous solution are modified to conditions favorable to stability, is fundamental. For example, in the highly saline conditions of Äspö waters, colloid generation is almost negligible, but intrusions of diluted water (glacial melt water) may induce clay disaggregation and formation of colloids.

Aggregation/disaggregation processes produced by the changes in ionic strength in smectite (the main component of the bentonite backfill) and 2:1 clay, illite were be studied by PCS and single particle counting (SPC).

The disaggregation process of smectite clays has been shown to be not completely reversible: in general, the aggregation process is very rapid (minutes) but it might be necessary much more time until a complete disaggregated state is reached (days-weeks). Very favorable electrolytes, like deionized water, accelerate the disaggregation process. The concentration of colloids in the suspension and the pH of the water are also points to be taken into account in the process evaluation.

3. Analysis of the effects of the presence of different anions on colloid stability.

The conditions required to consider colloids as *"stable"* are: **(1)** low ionic strength of the groundwater ($\leq 1 \cdot 10^{-3}$ M) and **(2)** pH far from the point of zero charge (pH_{PZC}). Parameters like the critical coagulation concentration, CCC, the pH_{PCZ} or the isoelectric point (pH_{IEP}) are adopted to define the stability of colloidal systems, but they might not be totally representative of the real behaviour of colloids in nature, as the presence of sorbable ions destabilize colloids at much lower concentration that *inert* ions. Ion adsorption and ion exchange in clays, may change colloid surface and even the water chemical composition.

In particular, the effect of inorganic anion adsorption on colloid stability is scarcely investigated. We evaluated the effects of the adsorption of inorganic anions on Al_2O_3 and bentonite colloid stability. Results showed that highly sorbing anions like selenium and sulphate clearly affects the stability of Al_2O_3 colloids at relatively low concentrations ($1 \cdot 10^{-4}$ M). At ionic strength of $1 \cdot 10^{-3}$ M and below pH<7 a different aggregation state is observed depending on the electrolyte ($ClO_4^- < NO_3^- < HCO_3^- < SO_4^{2-} \sim SeO_3^{2-}$). This aggregation state is related to the adsorption of the anion and the sorbate surface coverage.

The zetapotential measured Na-smectites prepared either in $NaClO_4$ or Na_2SO_4 at approximately $I=1 \cdot 10^{-3}$ M was negative in all the pH range, as expected for smectite, but slightly different: in Na_2SO_4 the zeta potential was approximately 10 mV higher (in absolute value). In spite of that, smectite was less stable at acidic pH in the presence of the sulphate. This is related to sulphates sorption on the =SOH edge sites of the smectite which decrease the edge-edge repulsions, similar to that observed for the alumina oxide. Under alkaline conditions, the smectite stability behaviour was quite similar independently of the electrolyte.

Acknowledgements

This work received funding from EU Seventh Framework Programme (FP7/2007-2011) grant agreement Nº 295487 (BELBAR, Bentonite Erosion: effects on the Long term performance of the engineered Barrier and Radionuclide transport).

RADIONUCLIDE SORPTION ON MX-80 BENTONITE COLLOIDS AND COLLOID ASSOCIATED RADIONUCLIDE TRANSPORT

Pirkko Hölttä[1*], Suvi Niemiaho [1], Outi Elo[1], Valtteri Suorsa [1]
[1] University of Helsinki, Laboratory of Chemistry (FI)

* Corresponding author: pirkko.holtta@helsinki.fi

Abstract

The potential relevance of colloids for radionuclide transport is highly dependent on their interaction with radionuclides. The objective of this work has been to study the radionuclide and colloid interaction by means of the batch sorption and column experiments. The transport of Sr-85 and Eu-152 in a fracture column and crushed rock columns was studied without and with colloids. The sorption of Sr-85 and Eu-152 on bentonite colloids depended on the ionic strength of the medium and the valence of the cations in the solution. The distribution coefficient (K_d) decreased when the ionic strength increased. Particularly Eu-152 but Sr-85 were strongly retarded in the fracture column and altered crushed rock column without colloids. In the presence of bentonite colloid suspension, the elution of radionuclides was obtained. The results showed the effect of the water flow rate and thus the residence time on the colloid recovery indicating colloid filtration in a fracture or crushed rock surfaces.

Introduction

Colloid-facilitated transport of radionuclides may significantly contribute to the long–term performance of a spent nuclear fuel repository. In Olkiluoto, the determined natural inorganic and organic colloid contents in groundwater are low – less than 1 ppm – but the bentonite buffer used in the EBS system is assumed to be a potential source of colloids. For colloid-facilitated transport it is essential that colloids must be generated, contaminants must associate with the colloids and colloids must be transported through the groundwater. Objective of this work is to study the radionuclide and colloid interaction with a rock in different groundwater conditions. The overview of ongoing experimental work and examples of preliminary results are given.

Experimental

The bentonite used is MX-80 Volclay type bentonite powder which consists mainly of montmorillonite. Colloid dispersion solution was made from MX-80 bentonite clay powder which was mixed with Milli-Q water. Allard, low salinity granitic ($I = 4.2\ 10^{-3}$ M) and diluted OLSO ($I = 0.517$ M) reference groundwater were used as solutions. OLSO simulates the current saline groundwater in Olkiluoto in oxic conditions. Electrolyte solutions, NaCl ($I = 1$ M – $1\ 10^{-7}$ M) and $CaCl_2$ ($I = 3$ M – $3\ 10^{-7}$ M) were used to study the effect of salinity. The fracture column from Olkiluoto tonalite drill core was artificially fractured along the natural fracture. The fracture width in the column was about 3.5 cm, the column length 6.8 cm and the fracture aperture 100 µm. The crushed rock columns were made of Kuru Grey granite and strongly altered tonalite from the Syyry area in Sievi. The column diameter was 1.5 cm and length 15 cm or 30 cm. Colloidal particle size distributions were determined applying the dynamic light scattering method and zeta potential applying the dynamic electrophoretic mobility (Malvern Zetasizer Nano ZS). Colloid concentration was determined using a standard series made from MX-80 bentonite and a derived count rate obtained DLS measurements. Colloid concentration

determination was verified by analyzing the aluminum content of montmorillonite using ICP-MS. In the sorption experiments, colloid solution was added to the solution spiked with Sr-85 or Eu-152 tracer, 4.7 mL aliquot were taken after 2 h, 1, 2 and 7 days and solid colloid fraction was separated by ultracentrifugation (90000 rpm/60 min). The gamma activity of Sr-85 or Eu-152 was detected from the separated liquid phase using a Wizard gamma counter. Sorption was quantified by the determination of the distribution ratio of radionuclide activity between solid and liquid phase. In the flow experiments, water was pumped through the fracture or crushed rock column at different flow rates of 5–25 μL min^{-1} using a peristaltic pump to control water flow rate. A short tracer pulse (20 μL) was injected into the water flow using an injection loop and the out flowing tracer was collected using a fraction collector and the radioactivity was measured.

Results and discussion

Radionuclide sorption onto bentonite colloids was quantified by batch experiments that give a distribution ratio (K_d) of radionuclide between solid and a liquid phase. Nearly all of Sr-85 and Eu-152 was rapidly sorbed onto bentonite colloids in 0.001 M solutions. Sorption was nearly 100 % and measured radioactivity in a liquid phase was at the background level resulting in inaccurate K_d determination. The obtained results confirmed the influence of ionic strength and Ca^{2+} concentration on the sorption of Sr-85 and Eu-152 onto bentonite colloids. In the column experiments, the retardation factor can be estimated from the breakthrough curves of the conservative tracer and the radionuclide when the same experimental conditions have been used. In the Olkiluoto fracture column and Syyry altered tonalite crushed rock column, particularly Eu-152 but also Sr-85 was strongly retarded without colloids. In the presence of bentonite colloid suspension, the slow elution of Eu-152 and Sr-85 was obtained. In the Kuru grey unaltered granite crushed rock column, slight effect of bentonite colloids was found in the breakthrough curves of Sr-85. No breakthrough of Eu-152 activity was detected during two week experiment without the addition of bentonite colloids. Bentonite colloid filtration in a fracture or crushed rock surfaces was observed and the migration of colloids was affected primarily by colloid size but also by the type of column and/or rock alteration.

Summary and Conclusions

The radionuclide and bentonite colloid interaction has been studied by the means of the batch sorption and column experiments. The obtained results confirmed the influence of ionic strength and Ca^{2+} concentration on the sorption of Sr-85 and Eu-152 onto bentonite colloids. Bentonite colloids were observed to have a significant influence on the migration of Sr-85 and Eu-152 in the fracture and crushed rock column experiments. Migration of bentonite colloids in columns was affected primarily by colloid size but also by water flow rate and column type.

Acknowledgement

This is part of EU/BELBaR project. The research leading to these results has received funding from the European Atomic Energy Community's Seventh Framework Programme (FP7/2007-2011) under grant agreement n° 295487.

STUDY OF ^{85}Sr TRANSPORT THROUGH A COLUMN FILLED WITH CRUSHED GRANITE IN PRESENCE OF BENTONITE COLLOIDS

Kateřina Videnská[1*], Radek Červinka [1]

[1] ÚJV Řež, a. s. (CZ)

* Corresponding author: Katerina.Videnska@ujv.cz

Abstract
The presented work is focused on study of strontium transport through crushed granite in presence of bentonite colloids in dynamic arrangement. The results showed different behaviour of bentonite colloids and strontium in column, the colloids behaved as non-sorbing tracer, the strontium showed strong sorption on granitic material.

Introduction

The main aim of experiments was to prepare stable radiocolloid suspension (^{85}Sr + bentonite colloids) and compare the strontium and radiocolloid suspension behaviour passing through crushed granite and quantification the effect of bentonite colloids presence on strontium migration (mobilization/immobilization). The migration experiments were investigated under dynamic conditions in column set-up which provides an approximation to real conditions, existing in the environment.

Experimental

Solid phase
Granitic rock was sampled from the bore core, originating from the depth 97.5-98.7 m (Melechov massif, Czech Republic). The crushed granite was sieved into defined fractions, fraction with grain size 0.125-0.63 mm was used for presented experiments.

Liquid phase
The $SrCl_2$ solution (c = 10^{-6} mol/l) spiked by ^{85}Sr in distilled water was used as liquid phase in static and dynamic experiments. The final solution activity was 0.7 kBq/cm^3. The colloid suspension was used as a liquid phase in dynamic experiments without presence of strontium. The colloids concentration was c = 100 mg/l. The purified bentonite "Bentonite 75" denoted as B75 in Na^+ form was used for clay colloids preparation. Initially the mean hydrodynamic size of bentonite particles in suspension was about 500 nm (PCCS measurement).

Radiocolloid suspension was prepared by mixing the specific volume of $SrCl_2$ solution (c = $2 \cdot 10^{-6}$ mol/l) spiked by ^{85}Sr as a tracer and same volume of bentonite colloids. The final strontium concentration in radiocolloid suspension was 10^{-6} mol/l and bentonite colloids concentration was 100 mg/l. The contact time between strontium and the colloid particles before the dynamic experiments was seven days to ensure equilibrium.

Sorption experiments
Sorption of strontium was studied by static batch method. The crushed granite and mica mineral were used as solid phases; 10^{-6} mol/l solution of $SrCl_2$ spiked by ^{85}Sr in distilled was used

as liquid phase. The mixture was shaken for 9 days, solid to liquid ratio was 1:20. The activity of strontium was measured in aqueous phase by gamma spectrometry.

Column experiments
The crushed granite was placed into 5 cm^3 plastic columns. The inlet of liquid phase into column was continuous with constant colloid concentration, strontium concentration and flow rate of liquid phase. Defined volume samples of liquid phase were taken in defined time intervals from the column outlet for the measurement colloids concentration and strontium activity. The transport of studied tracers through crushed granite is illustrated by breakthrough curve. The number of pore volume n_{PV} is on x-axis, the relative concentration (activity) c_{rel}, A_{rel} measured at outlet of column is on y-axis (Palágyi et al., 2013).

Results

Sorption experiments
Sorption of strontium on granite was studied by static batch method. The aim of static experiments was to estimate the extent of strontium sorption on individual minerals (especially mica mineral muscovite) of crushed granite. The crushed granitic rock itself and segregated muscovite were used as solid phase; the experiments were carried out with 10^{-6} mol/l solution of $SrCl_2$ spiked by ^{85}Sr in distilled water. The muscovite was considered as a possible dominant sorbent of strontium in granitic material. However this assumption was not confirmed, the results showed higher sorption of strontium on granite (K_d = 30 ml/g) than on muscovite (K_d = 20 ml/g).

Column experiments
The obtained beakthrough curves describing transport of each tracer are displayed in Figure 1. Firstly, the column experiments were conducted only with clay colloid suspension. The transport of colloids through crushed granite was fast, without retardation and comparable with behaviour of conservative, non sorbing tracer ^3H (▲).

Then the dynamic experiment with radiocolloid suspension was performed. The bentonite colloids in presence of ^{85}Sr (■) passed through crushed granite during first 24 hours and left the strontium (♦) in the column. The sorption potential of granite material was higher, than the forces of interaction between strontium and bentonite colloids (ion exchange). The strontium transport duration was about 20 days and 400 pore volume of aqueous phase flew through crushed granite. The observed retention of strontium on granite suggests higher affinity of strontium towards granitic rock than towards bentonite colloids and showed the reversibility of the sorption of strontium on bentonite colloids.

Finally, the column experiment with strontium without presence of colloid particles was carried out. The strontium behaviour was similar as during the experiment with radiocolloid suspension. Strontium sorption was also strong and strontium transport lasted even longer than strontium transport in the presence of colloids.
Observed strontium behaviour differed significantly from the strontium behaviour described in our previous experiments which studied strontium transport through crushed granite (●) (Palágyi et al., 2013). The strontium solution was prepared in synthetic granitic water (SGW). This experiment was completed after 3 days. Different strontium behaviour is probably caused by using various aqueous phases and possible competitive behaviour of cations (Ca^{2+}, Mg^{2+}) presence in SGW because concentrations of these cations were up to 100 times higher than the strontium concentration in experimental solution.

The breakthrough curves were fitted by CXTFIT Code (STANMODE, version 2.08). The input parameters were flow velocity v, dispersion coefficient D and retardation coeffi-

cient *R*. For initial estimate we used their experimental values and the values of *v* and *D* were fitted by CXTFIT Code (Toride et al., 1995).

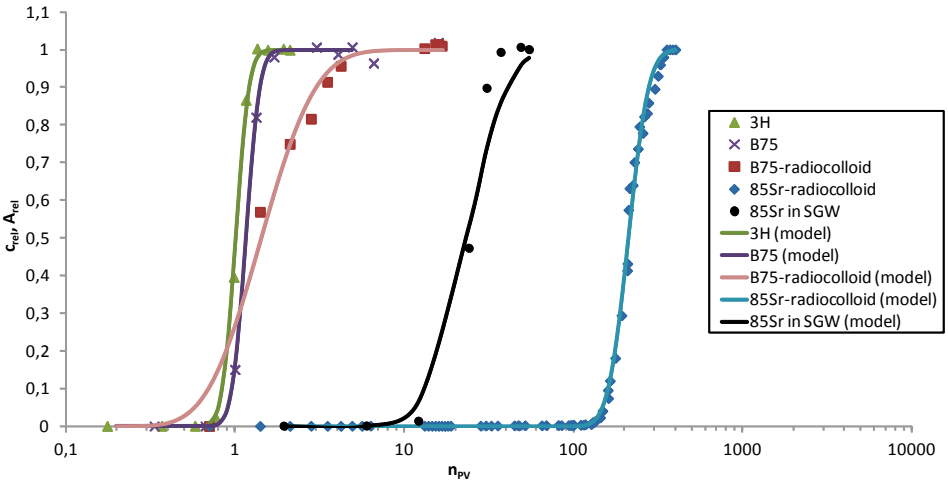

Figure 1: *Experimental (points) and model (lines) breakthrough curves of different tracers in crushed granite of 0.125-0.63 mm grain size.*

Summary and Conclusions

The strontium transport through crushed granite in presence of bentonite colloids has been studied by dynamic experiments under aerobic conditions. The transports of strontium and colloids were completely different. The colloid particles passed through column without retardation, colloids behaved as conservative, non-sorbing tracer (^{3}H). On the other hand strontium showed very strong sorption on crushed granite.

Acknowledgement

The research leading to these results has received funding from the European Atomic Energy Community's Seventh Framework Programme (FP7/2007-2011) under grant agreement 295487 – project BELBaR and from SÚRAO (CZ).

References

Palágyi Š., Štamberg K., Havlová V., Vodičková H. (2013). Effect of grain size on the $^{85}Sr^{2+}$ sorption and desorption in columns of crushed granite and infill materials from granitic water under dynamic conditions. .J Radioanal. Nucl. Chem., 297, 33-39.

Toride N., Leij F.J., van Genuchten M.Th. (1995). The CXTFIT Code for Estimating Transport Parameters from Laboratory or Field Tracer Experiments, version 2.0. Research Report No. 137, U.S. Department of Agriculture, Riverside, California.

RADIONUCLIDE/BENTONITE DISSOCIATION KINETICS

Nick Bryan[1*] and Nick Sherriff[1]

[1] University of Manchester, Manchester (U.K.)

* Corresponding author: nick.bryan@manchester.ac.uk

Introduction

Bentonite colloids could act as vector for the transport of radionuclides, but the probability of migration is expected to depend upon the reversibility of the interaction with radionuclides. Therefore, the dissociation rate constants for a series of radionuclides are being studied.

Results

Ternary systems of ^{152}Eu(III), bulk bentonite and EDTA ([Eu]=7.9 10^{-10} M; pH=6.0 – 7.0) have been studied. Without ligands, there was slow uptake in a two stage process, with initial rapid sorption of Eu(III), followed by slower uptake of a much smaller fraction (2.5%). The reversibility of Eu(III) binding was tested by allowing Eu(III) to sorb to bentonite for 1 – 322 days. EDTA was added to the pre-equilibrated Eu bentonite mixtures at a concentration (0.01 M) that was sufficient to suppress sorption in a system where EDTA was present prior to the contact of Eu(III) with bentonite. Some fraction of the Eu was released instantaneously, but a significant fraction remained bound. With time, the amount of Eu(III) remaining bound to the bentonite reduced, eventually with a rate constant of approximately 5. 7 x 10^{-8} s^{-1}(values in the range 3.7 x 10^{-8} – 1.0 x 10^{-7} s^{-1}). After an EDTA contact time of approximately 100 days, the amount of Eu(III) remaining bound to the bentonite was within error of that when EDTA was present prior to contact (4.5% ± 0.6). The amount of slowly dissociating Eu increased with increasing Eu(III)/bentonite pre-equilibration time up to approximately 25% over a pre-equilibration time of 100 days. Figure 1 shows the dissociation from the bulk bentonite, plotted as a function of pre-equilibration time.

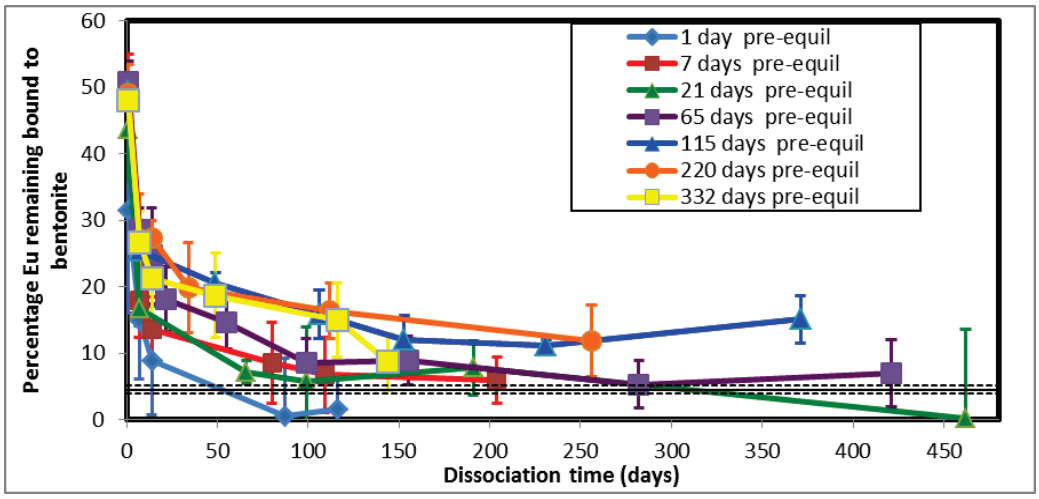

Figure 1: *Eu(III) dissociation from bentonite clay versus time in contact with EDTA as a function of Eu/bentonite pre-equilibration time. The black horizontal line represents the equilibrium distribution.*

There is evidence for a range of dissociation rate constants from instantaneously dissociating to the distinct most slowly dissociating fraction described above.

The dissociation of ^{152}Eu(III) from colloidal bentonite (150 ppm) was also studied, but this time using Dowex cation exchange resin as a competing sink. The dissociation data for these colloidal experiments are shown in Figure 2; this time plotted as the natural log of the percentage of Eu remaining bound to bentonite.

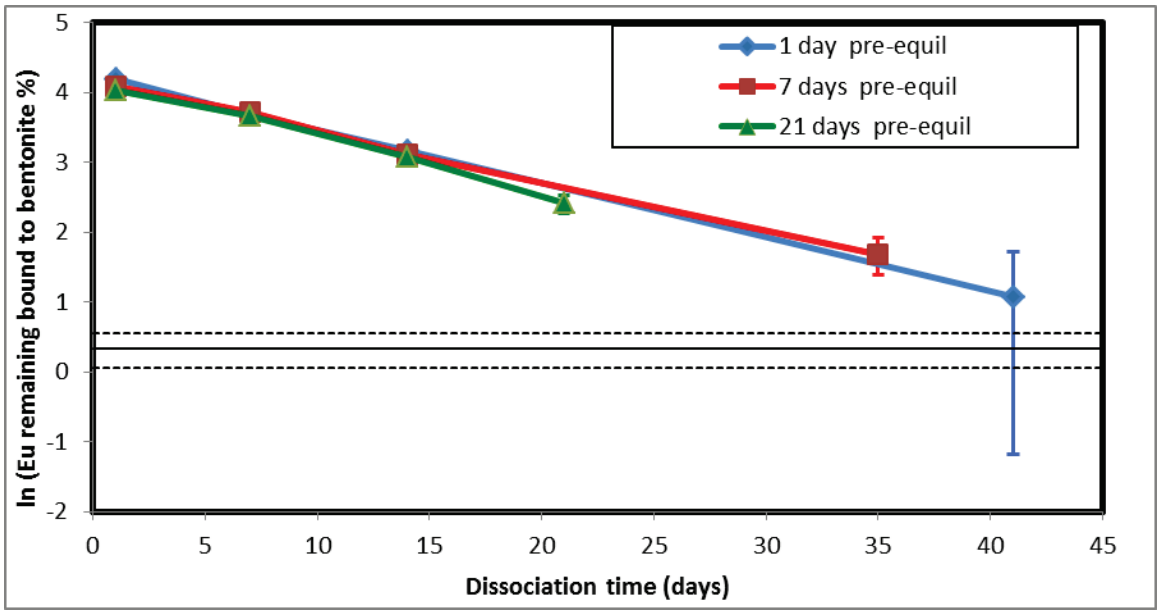

Figure 2: *natural log plot for the colloid dissociation experiment: ln(percentage bound to bentonite) vs Dowex contact times, as a function of pre-equilibration time. The black horizontal line represents the equilibrium distribution*

This time, the kinetics were much simpler, with just two fractions. There is an instantaneously dissociating fraction that accounts for approximately 30 – 35% of the Eu(III), but the remainder of the Eu dissociates with a single first order rate constant. The average rate constant from the data in Figure 2 is 8.9 x 10^{-7} s^{-1}(values in the range 8.3 x 10^{-7} – 9.5 x 10^{-7} s^{-1}; note the much tighter range this time).

Conclusions

Slow dissociation has been measured and quantified for bulk and colloidal bentonite systems. It has been found that dissociation from colloidal bentonite is significantly faster than for the bulk systems. Therefore, although there are some similarities in the behaviours, there are important differences between the two systems. In both bulk and colloidal bentonite systems, although slow dissociation from bentonite has been observed, there was no 'irreversible' uptake. Experiments with uranyl and thorium are also in progress.

NEW RESULTS FROM THE CFM PROJECT & CURRENT STATUS

T. Schäfer[1*], I. Blechschmidt[2], M. Bouby[1], S. Büchner[1], J. Brendlé[3], G. Darbha[1], H. Geckeis[1], T. Kupcik[1], R. Götz[1], W. Hauser[1], S. Heck[1], F. Huber[1], M. Lagos[1], F. Quinto[1], A. Martin[2]

[1] KIT, Institute for Nuclear Waste Disposal (INE), Karlsruhe, Germany
[2] NAGRA Natl. Cooperat. Disposal Radioact. Waste, Wettingen, Switzerland
[3] Lab. Mat. Mineraux, UMR CNRS, Univ. Haute Alsace, Mulhouse, France

* Corresponding author: thorsten.schaefer@kit.edu

Abstract

The influence of colloidal/nano-scale phases on the radionuclide (RNs) solubility and migration behavior is still one of the uncertainties in repository safety assessment [1]. In our work, we aim 1) to identify the presence and the formation of relevant colloids in repository specific areas, 2) to determine their stability as a function of geochemical parameters, 3) to elucidate the thermodynamics and kinetics of the colloid interaction with radionuclides, 4) to perform laboratory and field experiments to quantify the colloid mobility and their interaction with surfaces. The final goal is to state on the relevance of the nanoparticles (NPs) / colloids for the radionuclides migration in natural geochemical conditions. In this contribution we report on the progress concerning the colloid migration under near natural hydraulic conditions at the Grimsel Test Site. Within the Colloid Formation and Migration (CFM) project at the Grimsel Test Site (GTS Switzerland) [2] a huge geo-technical effort was taken to isolate hydraulically a shear-zone from the artificially introduced hydraulic gradient due to the tunnel construction. The construction is a combination of polymer resin impregnation of the tunnel surface and a steel torus to seal the tunnel surface. The steel tube with reinforcement rings is sealed at both ends with rubber based hydraulic "donut" packers and the annulus between resin and steel ring is filled and pressurized with water to counteract the hydrostatic pressure of the water conducting feature giving mechanical support to the resin. Natural outflow points of the MI shear zone were localized prior to the construction and sealed by surface packers. This design gives the opportunity to regulate outflow and thereby adjust the flow velocity in the fracture.

After optimization of the experimental setup and injection procedure through a number of conservative tracer tests using fluorescence dyes and so-called "homologue" tracer tests performed by injecting a suspension of Febex bentonite colloids associated Eu, Tb, Hf in addition to the conservative tracer a license was granted by the Swiss regulator (BAG) in 2012 to perform radionuclide tracer tests under these low-flow conditions.

Two injection cocktails of 2.25L volume were prepared at INE and transferred to GTS. A Febex montmorillonite clay colloid suspension of approx. 100 mg/L was used, whereas ~10% were present as synthetic montmorillonite with structural incorporated Ni. For details on the structural characterization of the Ni- montmorillonite phyllosilicate, see [3]. Beside the colloids and the conservative tracer Amino-G the radioisotopes ^{22}Na, ^{133}Ba, ^{137}Cs, ^{232}Th,^{233}U, ^{237}Np, ^{242}Pu and ^{243}Am were injected. The trivalent and tetravalent actinides were quantitatively associated with the colloids present as well as Cs, whereas Np(V), U(VI) and Na are not bentonite colloid bond.

Two separate experiments with injection (0.33 mL/min) of the radionuclide bentonite colloid cocktail were performed:

(1) Through borehole CFM 06.002-i2 into the MI shear zone and the water extracted under a constant flow rate of approx. 25 mL/min from the "Pinkel" surface packer (dipole distance 6.08m). (later referred as Run 12-02)
(2) Second injection through the "CRR dipole" into the MI shear zone [4] under lower flow rate than CRR at CRR 99.002-i2 (injection) and extraction at BOMI 87.010-i2 with a flowrate of 5 mL/min while keeping a constant flow rate of approx. 25 mL/min from the "Pinkel" surface packer (dipole distance 2.30m). (later referred as Run 13-05)

The tracer cocktail was recirculated in the injection loop to monitor the fluorescence decrease of the conservative tracer (Amino-G) and therefore providing an injection function for consequent transport modeling. For on-site colloid analysis a mobile Laser- Induced Breakdown Detection (LIBD) system similar to the one used in the CRR experiments [4] was transferred to Grimsel and installed in-line at the extraction side of the experiments to directly monitor the mobile colloid fraction throughout the experiment.

The conservative tracer Amino-G was recovered with recoveries >90% both by on site inline and off-site fluorescence detection. Analysis of Run 12-02 for the weakly sorbing tracers by γ-spectrometry performed by PSI-LES and INE showed very good conformity and revealed recoveries for ^{22}Na, ^{137}Cs and ^{133}Ba of 64%, 10% and 1%, respectively. LIBD determined recovery was quantified to be 48 ± 5%, whereas for the structural components Al and Ni detected by high resolution HR-ICP-MS a recovery of 44-49% and 51-52%, respectively, was quantified. The Al/Ni ratio in the injection cocktail was determined to be 21.6 and an average ratio of 20.4 ± 0.5 was found over the samples analyzed given clear evidence that a mobilization of Al containing phases as an additional colloid source from the fracture can be excluded.

Based on a number of colloid migration experiments performed in the MI shear zone a colloid attachment/filtration rate can be estimated, which is considerably lower than the value of $2 \cdot 10^{-2}$ estimated by filtration theory in [5]. All injected radionuclides including the strong sorbing tri- and tetravalent actinides could be detected in the eluent. The data of Run 12-02 and Run 13-05 obtained so far clearly show the mobility of bentonite derived montmorillonite colloids under near-natural flow conditions in the MI shear zone of the Grimsel Test Site [6,7]. The experimental data will be discussed in detail in the presentation together with new results using RIMS and AMS on the very slow reversible Pu fraction detected up to seven months in the tailing of the BTC's. Finally, the current set-up of the LIT (**L**ong-term **I**n situ **T**est) on bentonite erosion under natural conditions will be presented.

Acknowledgement

The research leading to these results has received funding from the German Federal Ministry for Economic Affairs and Energy (BMWi) under project 02E10679 & 02E11203B and partial funding under the 7th Framework Programme (FP7/2007-2011) project "BELBaR" under grant agreement 295487.

References

[1] T. Schäfer, et al. Appl. Geochem., 27 (2012) 390-403.
[2] H. Geckeis, et al., Actinide - Nanoparticle interaction: generation, stability and mobility, in: S.N. Kalmykov, M.A. Denecke (Eds.) Actinide Nanoparticle Research, Springer, 2011, pp. 1-33.
[3] Reinholdt, et al., Nanomaterials, 3 (2013) 48-69.
[4] H. Geckeis, et al., Radiochim. Acta, 92 (2004) 765-774.
[5] T. Schäfer & U. Noseck, Colloid/ Nanoparticle formation and mobility in the context of deep geological nuclear waste disposal (Project KOLLORADO; Final report), FZKA report 7515, 2010.
[6] F. Huber, U. Noseck, T. Schäfer, Colloid/nanoparticle formation and mobility in the context of deep geological nuclear waste disposal (Project KOLLORADO-2; Final report), KIT Scientific Reports 7645, 2014.
[6] www.grimsel.com

ACTINIDE(IV) COLLOIDS AT NEAR-NEUTRAL PH DUE TO REACTION WITH DISSOLVED SILICIC ACID

Harald Zänker, Stephan Weiss*, Christoph Hennig, Richard Husar

Helmholtz Zentrum Dresden Rossendorf, Institute of Resource Ecology (D)

* Corresponding author: S.Weiss@hzdr.de

Abstract

A new type of actinide(IV) colloids - silica-containing U(IV), Th(IV) and Np(IV) colloids formed in near-neutral solutions of background chemicals of geogenic nature (carbonate, silicic acid, Na^+) - was studied. Whereas the radiocolloids hitherto addressed in the BELBaR project are formed by the adsorption of radionuclides onto pre-existing particles, the colloids here under discussion result from a reaction of dissolved tetravalent actinides, An(IV), with dissolved silicic acid. An-O-Si bonds, which increasingly replace the An-O-An bonds of the amorphous actinide(IV) oxyhydroxide with increasing silica concentration, make up the internal structure of these colloids. The particles remain stable in aqueous suspension over years. A concentration of up to 10^{-3} M of colloid-borne An(IV) and a particle diameter of < 20 nm was observed. The question if such An(IV) colloids may contribute to the mobility of the actinides in the near-field or the far-field of a nuclear waste repository is discussed.

Introduction

Due to their low solubility, tetravalent actinides are often assumed to be immobile in natural waters. However, insoluble precipitation products can also be mobile if they occur as colloids. For An(IV) oxyhydroxides this phenomenon has thoroughly been studied in the past (e.g. Altmaier et al. (2004)). Recently, the formation of a another type of An(IV) colloids has been described (Dreissig et al. (2011), Hennig et al. (2013), Husar et al. (2013), Zänker and Hennig (2014)) - silica-containing U(IV), Th(IV) and Np(IV) colloids produced in near-neutral solutions of background chemicals of geogenic nature (carbonate, silicic acid, Na^+).

Laboratory experiments

Whereas the radiocolloids hitherto addressed in the BELBaR project are formed by the adsorption of radionuclides onto pre-existing particles (clay mineral particles), the colloids here in the focus result from a reaction of dissolved An(IV) with a geogenic component ubiquitous in bentonite and further compartments of a nuclear waste repository (dissolved silicic acid). In these colloids the actinides are bound by structural inclusion. The higher the concentration of dissolved silicic acid and the pH of the experimental solutions, the smaller and the more stable are the particles that are formed. An-O-Si bonds, which increasingly replace the An-O-An bonds of the amorphous actinide(IV) oxyhydroxide with increasing silica concentration, make up the internal structure of these colloids as was elucidated by EXAFS spectroscopy and further spectroscopic methods. The isoelectric point of the nanoparticles is shifted toward lower pH values by the incorporated silica. The particles remain stable in aqueous suspension over years. A concentration of up to 10^{-3} M of colloid-borne An(IV) was observed which is a concentration significantly higher than the concentrations of truly dissolved or colloidally sus-

pended waterborne An(IV) species hitherto reported for the near-neutral pH range. The prevailing diameter of the particles is below 20 nm (about 10 to 100 kDa). Phenomenologically, the mechanism of colloidal stabilization under discussion here can be compared with the so-called "sequestration" by silica, a phenomenon well known from trivalent heavy metal ions such as iron(III) (Robinson et al. (1992)) or curium(III) (Panak et al. (2005)) but never reported for tetravalent actinides before.

Geochemical implications

The question arises if such actinide(IV) colloids may occur in nuclear waste repositories after the access of water to the waste containers and their destruction and if these colloids may contribute to the mobility of the actinides in such cases. The following items deserve special attention. **(i)** There are several sources of silicic acid in a nuclear waste repository which could supply the silicic acid needed for colloid formation such as ingressing groundwater, corroding nuclear waste glass, cement or bentonite, injected grout silica. **(ii)** The formation of An(IV)-silica colloids in a nuclear waste repository cannot be ruled out since there are potential processes which might result in the formation of such colloids (decrease of the alkalinity of solutions containing An(IV) carbonate complexes and silicic acid, chemical or microbial reduction of An(V/VI) in the presence of silicic acid etc.) **(iii)** The An(IV)-silica colloids might prove to be relatively stable (resistant to coagulation) because both (a) a considerable repelling electrostatic force (i.e. a DLVO force) accompanied by a shift of the isoelectric point to lower pH values and (b) significant non-DLVO forces due to the increased influence of silica in the colloids play a role for the behavior of the actinide(IV)-silica colloids (cf. Hennig et al. (2013)). **(iv)** Transport of An(IV)-silica colloids through the engineered barrier system (compacted bentonite) and through the fractures of crystalline host rock cannot be ruled out since, for example, macromolecules of about 5 nm (lignosulfate, 30 kDa) were observed to diffuse through the pores of bentonite independently of the bentonite density (Wold and Eriksen (2003)) and the An(IV)-silica colloids may lie in the same size range.
Further research is needed to elucidate the potential role of actinide(IV)-silica colloids in environmental scenarios.

References

Altmaier M., Neck V., Fanghänel T. (2004). Solubility and colloid formation of Th(IV) in concentrated NaCl and $MgCl_2$ solution. Radiochimica Acta, 92, 537-543.

Dreissig I., Weiss S., Hennig C., Bernhard G., Zänker H. (2011). Formation of uranium(IV)-silica colloids at near-neutral pH. Geochimica et Cosmochimica Acta 75, 352–367.

Hennig C., Weiss S., Banerjee D., Brendler E., Honkimäki V., Cuello G., Ikeda-Ohno A., Scheinost A.C., Zänker H. (2013). Solid-state properties and colloidal stability of thorium(IV)-silica nanoparticles. Geochimica et Cosmochimica Acta 103, 197–212.

Husar R., Weiss S., Zänker H., Bernhard G. (2013). Investigations into the formation of neptunium(IV)-silica colloids. Migration 2013. Brighton, Book of Abstracts, 384.

Panak P.J., Kim M.A., Klenze R., Kim J.I., Fanghänel T. (2005). Complexation of Cm(III) with aqueous silicic acid. Radiochimica Acta 93, 133-139.

Robinson R.B., Reed G.D., Frazier, B. (1992). Iron and manganese sequestration facilities using sodium-silicate. Journal of American Water Works Association 84, 77-82.

Wold S., Eriksen T.E. (2003) Diffusion of lignosulfonate colloids in compacted bentonite. Applied Clay Science 23, 43-50.

Zänker H., Hennig C. (2014). Colloid-borne forms of tetravalent actinides: A brief review. Journal of Contaminant Hydrology 157, 87–105.

COAGULATION BEHAVIOUR OF CLAY DISPERSIONS IN PRESENCE OF VARIOUS CATIONS, ANIONS & ORGANIC MATTER

Radek Červinka[1*], Jenny Gondolli [1]

[1] ÚJV Řež, a. s. (CZ)

* Corresponding author: radek.cervinka@ujv.cz

Abstract

The coagulation experiments with dilute clay suspensions were performed mainly for prediction of colloids stability during the transport in the deep geological repository (DGR) far field. Influences of various cations, anions and organic substances on critical coagulation concentration (CCC) of clay suspensions were studied.

Introduction

The basic coagulation of dilute clay dispersions by inorganic cations (Na^+, K^+, Ca^{2+}, Mg^{2+}), anions (Cl^-, NO_3^-, SO_4^{2-}, PO_4^{3-}, OH^-) and organic substances (humic acid) was studied. Three clay dispersions (0.005 %, 0.05 % and 0.5 % w/w, i. e. 0.05, 0.5 and 5 g/l) of purified bentonite "Bentonite 75" denoted as B75 in Na^+ form were used. For comparison raw bentonite "Bentonite and Montmorillonite" denoted as BaM of similar origin as purified bentonite was selected. The Czech concept of DGR considers the granite as a host rock and the hydrochemistry of groundwater from this granitic environment was summarised in Czech report (Rukavičková et al., 2009). Three types of groundwaters were identified in granitic Bohemian Massif: groundwater – meteoric water in contact with granite (depths 30-100 m), mineral groundwater – meteoric water in contact with granite and deep CO_2 and fossil groundwater – old saline waters (see Table 1). The main aim of experiments was to determine the CCC for appropriate electrolyte solutions and compare the results with the chemistry of granitic groundwaters to decide about stability of bentonite colloids in these groundwaters.

Test-tube coagulation tests

Cations

The CCC of univalent cations (Na^+, K^+) and divalent cations (Ca^{2+}, Mg^{2+}) were determined in the series of test-tube coagulation tests for three bentonite suspension concentrations (0.005 %, 0.05 % and 0.5 % w/w) and different electrolyte (NaCl, KCl, $CaCl_2$ and $MgCl_2$) concentrations. The final solutions pH varied from 6.0 to 7.4. The coagulation was tested according to the procedure described in Berg (2010): 30 minutes after the mixing and 24 hours after the remixing of the suspension and more using visual inspection and laser light beam. Finally the presence/absence of particles in the upper part of dispersion was confirmed by photon cross correlation spectroscopy (PCCS) at Nanophox instrument (Sympatec GmbH, DE). The obtained CCC for cations and bentonite suspensions are summarised in Table 1.

Table 1: *Summary of results from coagulation experiments and comparison with chemical composition of different groundwaters. SGW – synthetic granitic groundwater used as a liquid phase for various experiments, others see text.*

Component		**Na**	**K**	**Ca**	**Mg**	**F**	**Cl**	**SO_4**	**HCO_3**	**NO_3**
SGW	**mg/l**	10.6	1.8	27.0	6.4	0.2	42.4	27.7	30.4	6.3
	mmol/l	0.5	0.0	0.7	0.3	0.0	1.2	0.3	0.5	0.1
Groundwater	**mg/l**	11.4	2.3	30.1	8.0	-	11.7	34.1	85.4	-
(median, n > 351)	**mmol/l**	0.5	0.1	0.8	0.3	-	0.3	0.4	1.4	-
Mineral groundwater	**mg/l**	501.5	25.5	60.9	28.7	-	92.6	162.5	1220.5	-
(median, n = 16)	**mmol/l**	21.8	0.7	1.5	1.2	-	2.6	1.7	20.0	-
Fossil groundwater	**mg/l**	1050.0	52.5	55.9	22.0	-	644.0	26.3	863.0	-
(median, n = 15)	**mmol/l**	45.7	1.3	1.4	0.9	-	18.2	0.3	14.1	-
CCC for selected cations		**Na**	**K**	**Ca**	**Mg**					
0.5 % w/w	**mg/l**	138-161	157-196	40-100	24-61	-	-	-	-	-
	mmol/l	6-7	4-5	1-2.5	1-2.5	-	-	-	-	-
0.05 % w/w	**mg/l**	138-161	117-157	4-20	12-24	-	-	-	-	-
	mmol/l	6-7	3-4	0.1-0.5	0.5-1	-	-	-	-	-
0.005 % w/w	**mg/l**	115-138	78-117	4-20	2-12	-	-	-	-	-
	mmol/l	5-6	2-3	0.1-0.5	0.1-0.5	-	-	-	-	-

Note: n = number of real groundwater analyses

Anions

In case of anions the 0.005% w/w bentonite suspension was used. For electrolytes NaCl, $NaNO_3$, Na_2SO_4 the appropriate CCC were 5, 6 and 3 mmol/l with corresponding ionic strength 5, 6 and 7.5 mmol/l. For $MgCl_2$, $Mg(NO_3)_2$ and $MgSO_4$ the CCC were exactly the same (0.5 mmol/l). For the Na_3PO_4 electrolyte, the coagulation (and CCC) was not found in the concentration range expected in the granitic groundwaters – this range was set to the values from 0.5 to 100 μmol/l according to the analyses of real groundwater samples and the bentonite leachates. Also the effect of varying pH in alkaline solutions on CCC was tested for the clay suspension (0.05% w/w). The pH varied from approx 8 to approx 13 to simulate the effect of alkaline solution coming from the concrete materials of DGR. The source of higher pH were NaOH and KOH, hence the effect of high Na and K concentrations in the solution have to be taken into consideration in CCC evaluation. The rising pH (from approx 8 to 12) does not have any significant effect on particles coagulation at given conditions.

Humic acid

CCC of univalent cations (Na^+) in presence of HA were determined in the series of test-tube coagulation tests for one bentonite suspension concentration (0.005% w/w) and different NaCl electrolyte concentrations (10 to 500 mmol/l) and HA concentrations (0 to 2 mg/l of total organic carbon (TOC)). The final solutions pH varied from 5.9 to 6.7. Same test procedure was used as for cations. The CCC for clay suspension in presence of NaCl electrolyte linearly increases with addition of HA. For higher concentration of HA the linear trend may not be valid as it is described in Borgino (2013), where linearity is maintained for HA concentration up to 10 mg/l for Fe(III)-montmorillonite.

Coagulation kinetics experiments

The coagulation kinetics of clay dispersion (0.005% w/w) in presence of NaCl electrolyte (10, 50 and 100 mmol/l) and HA (0 to 2 mg/l of TOC) was studied by PCCS starting with well-

dispersed system and following the increase in average hydrodynamic radius with time as the particles undergo coagulation. The hydrodynamic particle radius was monitored over time period of 1 hour recording the cross-correlation function every 3 minutes (1 minute of measuring and 2 minutes of pause). For data evaluation the method of 2nd cumulant was used. The CCC for system only with NaCl electrolyte (without HA) was measured between 3-10 mmol/l (see Figure 1). It is comparable with previous test-tube coagulation tests results. Below the CCC the mean hydrodynamic size do not change with time; above CCC the mean hydrodynamic size increases with time. The size change in a given time is dependent on electrolyte concentration. During the first 30 min. the size change is fast (fast coagulation) and decreases with time. After one hour the mean hydrodynamic size is quite similar for all electrolyte concentrations and particles aggregation is slow. For NaCl concentration > 10 mmol/l and experimental clay suspension the mean hydrodynamic size fluctuates in quite high range. The coagulation rate is probably so fast, that very large aggregates are created next to smaller one and this cause the high variations in the size. The presence of HA significantly increases the colloidal stability of bentonite particles, which also means, that in presence of HA the more concentrated NaCl electrolyte is needed for coagulation of clay dispersion (the CCC is higher). This effect seems to be primarily due to the reversal of edge surface charge from positive to negative, thereby preventing edge-to-face interactions. Very probably the HA is adsorbed on the clay edge surfaces due to the surface complexation between clay aluminol and HA carboxyl groups (Kretzschmar et al., 1998).

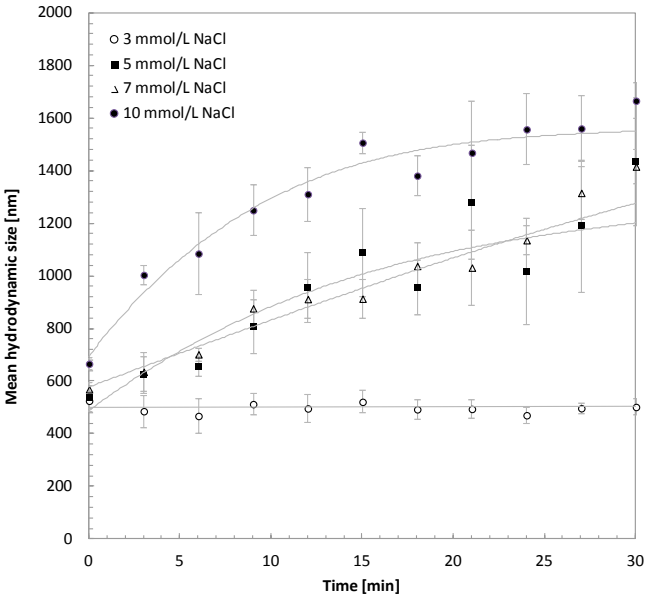

Figure 1: *Coagulation kinetics of clay suspensions (0.005 wt. %) in presence of different concentration of NaCl electrolyte, points with 1σ error bars and trend.*

Summary and Conclusions

Comparison of obtained CCC values for cations with concentrations of these cations in different types of granitic groundwaters lead to the conclusion, that these groundwaters are not suitable for stability of clay colloids even for dense bentonite suspensions (see Table 1). This was confirmed by test of clay colloids stability in SGW. Also the same coagulation tests in SGW for raw bentonite BaM demonstrated almost identical results as for B75 in Na^+ form. Colloid particles in these groundwaters coagulate and settle.

Acknowledgement

The research leading to these results has received funding from the European Atomic Energy Community's Seventh Framework Programme (FP7/2007-2011) under grant agreement 295487.

References

Berg, J. C. (2010). An Introduction to Interfaces and Colloids: The Bridge to Nanoscience. World Scientific Publishing Co. Pte. Ltd., Singapore, 785 pp.

Borgnino, L. (2013). Experimental determination of the colloidal stability of Fe(III)-montmorillonite: Effects of organic matter, ionic strength and pH conditions. Colloids and Surfaces A: Physicochem. Eng. Aspects., 423, 178– 187.

Kretzschmar, R., Holthoff, H., Sticher, H. (1998). Influence of pH and Humic Acid on Co-agulation Kinetics of Kaolinite: A dynamic Light Scattering Study. J. Colloid Interface Sci., 202, 95-103.

MODELLING SLIT EROSION EXPERIMENTS

Veli-Matti Pulkkanen[1*], Markus Olin[1]

[1] VTT Technical Research Centre of Finland (FIN)

* Corresponding author: veli-matti.pulkkanen@vtt.fi

Abstract

Modelling the so-called slit erosion experiments conducted in Work Package 2 has been approached with two concepts.

First, a modified version of the chemical erosion baseline model by ***Neretnieks et al. (2009)*** has been utilized in a number of model setups with different dimensions, flow velocities and salinities. The dependence of bentonite gel viscosity on the bentonite volume fraction has been limited to values below 700 and 45 000 times the lowest value and the complex functional dependencies have been replaced by piecewise polynomial interpolants to achieve better convergence when solving the model numerically (see ***Olin (2014)*** for details). The results show relation $Q \sim (vR)^n$ in both cases between the erosion mass flux Q, the flow velocity v, and the radius of the bentonite source R; the exponent was fitted to be 0.45 and 0.31 in the low and high limit cases, respectively. Qualitatively observing, the salinity of water seems to have a smaller effect on the swelling behaviour of bentonite in the model than in experiments. Moreover, the shape of the swollen bentonite in the model differs significantly from the shape in the slit erosion experiments. When reviewing the results, the difficulties in reaching convergent numerical solutions caused by the extremely steep gradients in parameters built in the model should be kept in mind.

The objective for the second approach has been to develop a model concept for bentonite that covers the range of phenomena seen in the slit erosion experiments: swelling from a solid material to a gel due to wetting, swelling due to the salinity changes and the breakdown of the structure of gel to eroding sol carried away by flowing water. Also, the model should not be a purely theoretical one but rely instead on experiments both in concepts and parameters.

The development of the model has been begun with the unsaturated solid bentonite, since this is the starting point in the most slit experiments. The widely used geotechnical models for unsaturated soils based on the concept of suction and on the use of extended Darcy's law for water movement together with extended Cam-Clay models for mechanical behaviour had to be abandoned, because the mismatch between the concepts and the phenomena in bentonite makes extending these models rather difficult. For example, the concept of diffusion should be used instead of suction extended Darcy's law, due to the molecular level bindings of water in bentonite interlayers. Also, the correlations between suction and mechanical properties should be replaced by simpler relations.

As well known, the chemical potential of water adsorbed to bentonite can be measured by balancing it with water vapour and stating that the potentials of them are the same. The diffusion velocity of water is proposed here to be the gradient of this potential multiplied by a transport coefficient, what is in accordance with the general concept of diffusion. The total

diffusion flux is then obtained by taking into account also the water density, the bound water volume per total volume and the effect of geometry.

The adsorption isotherms are often measured for unconfined clay samples (e.g. powders) for practical reasons, but the isotherms of confined samples differ from these ones. The reduction of the bound water chemical potential in confined samples has been found to correlate approximately to the product of swelling pressure and water volume by e.g. ***Kassiff and Shalom (1971)***, ***Kahr et al. (1992)*** and ***Dueck and Börgesson (2007)***. Here, this relation is used to correct the diffusion potential of confined samples but in integrated (and mechanically more general) form to make the free energies of the systems match instead of the potentials at certain water content.

The above relation also provides the coupling of the mechanical model to the bound water content through the underlying assumption of the bentonite volume change being the same as the volume of the bound water. This assumption is supported by ***Cases et al. (1992, 1997)*** and ***Bérend et al. (1995)***) who have found the bound water (in equilibrium with water vapour) to be adsorbed mainly to the interlayers of montmorillonite and by ***Delage et al. (1998)*** who show experimentally that the bound water increases the volume of clay (FoCa7 clay) by the volume of the water.

When the diffusion of the bound water is coupled to the volume change of bentonite, a simple hydro-mechanical model is obtained. To describe the behaviour when wetting by liquid water and the swelling by lowering salinity, also water in the free pore space (i.e. not the bound water) has to be included in the model. The movement of this water can be described by Darcy's law extended by the capillary effect, because of the free porosity pore sizes of compacted bentonite. The free water adds no volume of bentonite (it fills only empty porosity) but can loosen the structure of bentonite. On the other hand, the concentration of dissolved species can change the amount of bound water and swelling stress by altering the free water activity (i.e. the chemical potential) which in turn affects the bound water chemical potential similarly as water vapour (see e.g. ***Karnland (1998)*** and ***Karnland et al. (2003)***).

The transformation of solid bentonite into a gel is built in the mechanical model, in which the parameters change according to the dry density and salinity changes. To our knowledge, however, no systematic experiments on the mechanical properties of bentonite with different densities, water contents and salinities have been conducted. Without such results, the model cannot be called a model for a certain bentonite but only a model framework. Therefore, conducting the necessary experiments ourselves is being considered at the moment.

According the current model concept, the swelling of bentonite stops when an equilibrium between the mechanical energy (affected by the intrinsic mechanical properties of bentonite and the wall friction) and the chemical potential difference of bound and free water is reached. If the salinity of water decreases, the chemical potential difference increases and the bentonite gel structure may loosen inducing chemical swelling of bentonite.

The breakdown mechanism of bentonite gel is a topic for modelling in year 2015.

Acknowledgement

The research leading to these results has received funding from the European Atomic Energy Community's Seventh Framework Programme (FP7/2007-2011) under Grant Agreement no295487, the BELBaR project.

References

Bérend, I., Cases, J. M., Francois, M., Uriot, J. P., Michot, L., Masion, A., Thomas, F. (1995). Mechanism of Adsorption and Desorption of Water Vapor by Homoionic Montmorillonites. 2. The Li^+, Na^+, K^+, Rb^+ and Cs^+-Exchanged Forms. Clays and Clay Minerals, 43, 324-336.

Cases, J. M., Bérend, I., Besson, G., Francois, M., Uriot, J. P., Thomas, F., Poirier, J. E. (1992). Mechanism of Adsorption and Desorption of Water Vapor by Homoionic Montmorillonite. 1. The Sodium-Echanged Form. Langmuir, 8, 2730-2739.

Cases, J. M., Bérend, I., Francois, M., Uriot, J. P., Michot, L., Thomas, F. (1997). Mechanism of Adsorption and Desorption of Water Vapor by Homoionic Montmorillonites. 3. The Mg^{2+}, Ca^{2+}, Sr^{2+}, Rb^+ and Ba^{2+} Exchanged Forms. Clays and Clay Minerals, 45, 8-22.

Delage, P., Howat, M.D., Cui, Y.J. (1998). The relationship between suction and swelling properties in a heavily compacted unsaturated clay. Engineering Geology, 50, 31-48.

Dueck, A., Börgesson, L. (2007). Model suggested for an important part of the hydro-mechanical behaviour of a water unsaturated bentonite. Engineering Geology, 92, 160-169.

Kahr, G., Kraehenbuehl, F., Stoeckli, H.F., Müller-Vonmoos, M. (1990). Clay Minerals, 25, 499-506.

Karnland, O. (1998) Bentonite swelling pressure in strong NaCI solutions - Correlation of model calculations to experimentally determined data. Posiva Report 98-01, Posiva Oy, Olkiluoto, Finland

Karnland, O., Muurinen, A., Karlsson, F. (2003). Bentonite swelling pressure in NaCl solution — experimentally determined data and model calculations. In: Alonso, E.E., Ledesma, A. (Eds.), Proc. of the International Symposium on Large Scale Field Tests in Granite, Sitges.

Kassiff, G., Shalom, A. B. (1971). Experimental Relationshiop Between Swell Pressure and Suction. Géotechique, 21, 245-255.

Neretnieks, I., Liu, L., Moreno, L. (2009). Mechanisms and Models for Bentonite Erosion. Report SKB TR-09-35, Svensk Kärnbränslehantering AB, Stockholm, Sweden

Olin, M (2014). Tunnel Backfill Erosion by Dilute Water. Posiva Working Report 2014-07, Posiva Oy, Olkiluoto, Finland

STATUS UPDATE ON THE MODELLING WORK

Florian Huber & Thorsten Schäfer

Karlsruhe Institute of Technology (KIT), Institute for Nuclear Waste Disposal (INE),
P.O. Box 3640, 76012 Karlsruhe

* Corresponding author: florian.huber@kit.edu

Abstract

Within WP 5 KIT-INE will focus on the effect of natural fracture geometry on bentonite erosion and bentonite colloid transport. In detail, the work concentrates on the following:

1) **Effect of natural fracture geometry on bentonite erosion**

Firstly, 3D computational fluid dynamics (CFD) simulations (using Ansys Fluent) on 2 natural single fractured drill cores from Äspö, Sweden have been conducted. Both cores are characterized by µ-computed tomography (µCT) to obtain geometrical information on the fracture geometry and aperture distribution. The fracture geometry is used directly to generate a computational mesh for the 3D CFD simulations. Flow field calculations are varied as a function flow velocity to cover a range of natural occurring flow velocities in fractured ground water environments. Subsequently, the calculated flow fields together with the aperture fields of the fractures are used to calculate variability in bentonite erosion rates using the approach presented in Moreno et al. ***(SKB, 2010)***.

Secondly, the most comprehensive and frequently applied model for buffer and backfill erosion by Neretnieks et al. ***(SKB, 2009)*** has been implemented in 2D in the finite element code COMSOL Multiphysics both by KTH and, in a slightly simplified way, by VTT ***(Itälä et al., 2010)***. It has been planned to couple the erosion model (VTT model) to the KIT-INE 3D fracture models mentioned above. Due to the computational burden to use the full 3D model in conjunction with numerical problems/instabilities in solving the erosion model within COMSOL this approach seems not feasible. Alternatively, the use of simplified fracture flow fields in COMSOL based on the Cubic Law and the fracture aperture fields available would at least reduce the computational burden while the numerical problems of the erosion model would still be valid. First tests on the feasibility of this approach are underway.

2) **Bentonite colloid transport modelling**

To examine bentonite colloid transport in fractures both on an experimental and modelling basis, a flow cell with an artificial granodiorite fracture from Grimsel, Switzerland is produced. This flow cell will be used to study bentonite colloid migration as a function of aperture, flow velocity and ground water chemistry. The spatial distribution of the mineralogy on the fracture planes will be mapped (restricted to three different minerals, namely feldspar/plagioclase, quartz and mafic minerals) and explicitly incorporated in the model. By combining colloid attachment probabilities measured with Atomic Force Microscopy (AFM) for the mapped mineral phases at the fracture surface chemical heterogeneity is approximated in the simulations. Experimentally obtained colloid breakthrough curves will be modelled using either the Discrete Phase Model module within Ansys Fluent and/or the Particle Tracing

module within COMSOL Multiphysics. Until now, scoping transport experiments using fluorescence tracers (Amino-g and Rhodamin-b) in a Plexiglas dummy flow cell have been conducted.

References

Itälä, A., Seppälä, A., Pulkkanen, V.M., Olin, M., 2010. Smectite Expansion into Seeping Water (BESW). VTT-R-07924-10. 20 p.

SKB, 2009. Mechanisms and models for bentonite erosion. SKB Technical report TR-09-35. Svensk Kärnbränslehantering AB, Stockholm, Sweden.

SKB, 2010. Modelling of erosion of bentonite gel by gel/sol flow. Svensk Kärnbränslehantering AB, Stockholm, Sweden.

BENTONITE EXPANSION AND EROSION- DEVELOPMENT OF A TWO-REGION MODEL

Ivars Neretnieks*, Luis Moreno, Longcheng Liu

Dep. of Chemical Engineering, Royal Institute of Technology, KTH, Stockholm, SWEDEN

* Corresponding author: niquel@kth.se

Abstract

Erosion of smectite in a fracture intersecting a deposition hole for spent nuclear fuel with a clay buffer has been modeled with the dynamic clay expansion model using some simplifications compared to the previously used fully coupled model. A two-region model, which avoids some problems in earlier work was developed and tested. The model divides the region of the expanding clay in the fracture in one where the clay behaves like a Bingham solid/fluid that cannot flow but can expand by the repulsive forces between the smectite particles and another, the rim region surrounding the former where the gel/sol, although highly viscous in some locations, can flow and carry away the smectite particles that diffuse into this region. The rim region is very thin compared to size of the inner region. This two-region model gives results that are more accurate in some important regions than those obtained earlier by the fully coupled model because of a much higher resolution in the region where the erosion loss occurs.

Solution of the two-region model is obtained by first solving the rim model. This results in a simple expression for the given chemistry and smectite particle size and then depends only on the radius to the rim, fracture aperture and water velocity. The equations for the inner region are solved using a finite difference method having the rim model as a boundary condition to follow the expansion of gel into the fracture and how part of it is swept away at the rim. The numerical model uses an expanding grid with very fine discretization close to the rim and time stepping with increasing time steps. The numerical method is reasonably stable but sometimes can be quite time consuming with computing times reaching minutes to tens of minutes on a common desk top computer.

Another simpler method to solve the set of coupled equations based on a pseudo steady state approximation was also developed. It is very simple and uses analytic expressions that can be integrated by standard numerical integration methods when one wants to follow the evolution in time and space of the expanding front with the rim. This is called the pseudo steady state solution, PSS. To calculate the expansion and loss at the rim at steady state, a very simple equation results. The PSS solution was found to be able to bracket the numerical solution within a factor less than two. The two solution techniques mutually support each other.

In some examples covering a wide range of conditions relevant for a repository in crystalline rock it was found that the two-stage model, which solves the model equations considerably more accurately than what is obtained with the finite element modeling used earlier, gives considerably lower steady state losses of smectite. However, the clay expands much farther out in the fractures than previously found, which leads to a larger amount of clay residing in the fractures as the rim reaches a considerably larger distance. In all, the loss is smaller than previous results suggest. A further benefit is that as the smectite expands farther from the deposition hole, even in the finest fractures, it creates an extensive non-flow region around the deposition hole and tunnels. This considerably decreases the overall mass transfer rate of solutes to and from the deposition hole.

THEORETICAL STUDIES WITH DENSITY FUNCTIONAL THEORY (DFT) ON CA/ NA MONTMORILLONITE: STRUCTURE, FORCES AND SWELLING PROPERTIES

Guomin Yang, Longcheng Liu*, Ivars Neretnieks, Luis Moreno

KTH, *Royal Institute of Technology* (SE)

* Longcheng Liu: lliu@ket.kth.se

In Sweden, the KBS-3 disposal concept for storing high-level nuclear waste is to enclose the nuclear waste in a copper canister, as shown in Figure 1, which is embedded by the compacted bentonite deep underground**.**

The success of such containment depends, therefore, crucially on the stability of the clay buffer material consisting mainly of lamellar montmorillonite. The natural Na-bentonite of Wyoming type (MX-80), as shown in Figure 2 (a), consisting mainly of montmorillonite, as shown in Figure 2 (b), has a swelling capacity when it is in contact with groundwater. In this or similar situations, the electric double layer plays a decisive role in determining the swelling properties and the colloidal stability. This swelling property together with its low permeability sustains the Na-bentonite as an ideal candidate for the buffer and backfill material in the deep repository of nuclear waste in the Swedish KBS-3 disposal concept for spent nuclear fuels.

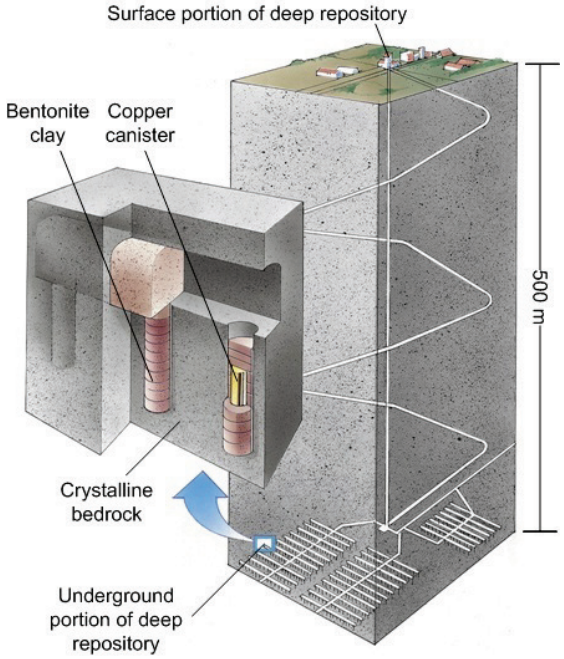

Figure 1: *Swedish KBS-3 repository design*

(a) MX-80 (Na-bentonite)

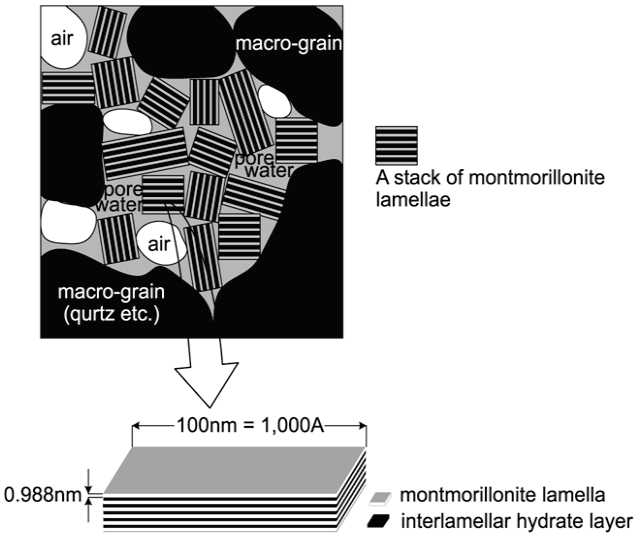

(b) Stacks of montmorillonite

Figure 2. *Bentonite buffer material*

In the erosion project we found that calcium bentonite properties and behaviour is poorly understood. In contrast to sodium bentonite in which the double layer forces are fairly well described by the Poisson-Boltzmann equation the calcium bentonite behaviour is strongly influenced by ion correlation and other effects not present in sodium dominated systems. One noticeable effect in calcium systems is that the smectite sheets tend to aggregate in stacks forming larger particles that are much less mobile than the individual sheets when separated. Another effect is that at high calcium concentrations in water the stacks seem to form a cohesive gel or at least do not seem to readily release particles upward in a downward facing gravity field.

We have started to look into the ion correlation effects and think that it should be possible to devise practically useful models for the behaviour of at least idealised calcium smectite sheets and stacks. We also have some evidence that the stacking of some but not all particles may be caused by charge heterogeneity of the smectite sheets as well as other heterogeneities.

Ca/Na montmorillonite properties have been studied theoretically using the density functional theory (DFT). For a clay system in equilibrium with pure water, the structure, swelling and thermodynamic properties have been characterised within the framework of the restricted primitive model (RPM). The diffuse double layer (DDL) with only counterions could be regarded as the simplest system to investigate DFT models, although it has been rarely applied by the available approaches within the framework of DFT. Under a wide range of conditions, ion density distributions and interactions between two charged sheets have been computed. When the clay counterions are monovalent, DFT simulations predict a considerable swelling, while in presence of divalent counterions attractive forces are obtained between the clay platelets with sheet distances near 1nm. This limited swelling of clay in the case of divalent counterions is a consequence of ion-ion correlations due to the ion size effect which becomes significant in strong coupled cases. Montmorillonite containing both Na^+ and Ca^{2+} counterions in contact with pure water will only show a modest swelling unless the fraction of surface charge neutralized by the Na^+ counterions is larger than 20-30%. The theoretical predictions of DFT simulations are in excellent agreement with both Monte Carlo simulations and experimental results.